PRODUCTION OF CARBON NANOTUBES BY CHEMICAL VAPOR DEPOSITION

A THESIS SUBMITTED TO
THE GRADUATE SCHOOL OF NATURAL AND APPLIED SCIENCES
OF
THE MIDDLE EAST TECHNICAL UNIVERSITY

BY

UMUT BARIŞ AYHAN

IN PARTIAL FULFILLMENT OF THE REQUIREMENTS
FOR
THE DEGREE OF MASTER OF SCIENCE
IN
CHEMICAL ENGINEERING

JULY 2004

Approval of the Graduate School of Natural and Applied Sciences

Prof. Dr. Canan Özgen
Director

I certify that this thesis satisfies all the requirements as a thesis for the degree of Master of Science.

Prof. Dr. Timur Doğu
Head of Department

This is to certify that we have read this thesis and that in our opinion it is fully adequate, in scope and quality, as a thesis and for the degree of Master of Science.

Assoc. Prof. Dr. Burhanettin Çiçek Co-Supervisor	Prof. Dr. Güngör Gündüz Supervisor

Examining Committee Members

Prof. Dr. Önder Özbelge (METU, CHE) _____

Prof. Dr. Güngör Gündüz (METU, CHE) _____

Prof. Dr. Şakir Erkoç (METU, PHYS) _____

Prof. Dr. Hayrettin Yücel (METU, CHE) _____

Prof. Dr. Üner Çolak (HU, NEM) _____

I hereby declare that all information in this document has been obtained and presented in accordance with academic rules and ethical conduct. I also declare that, as required by these rules and conduct, I have fully cited and referenced all material and results that are not original to this work.

Name, Last name : Umut Barış Ayhan

Signature :

ABSTRACT

PRODUCTION OF CARBON NANOTUBES BY CHEMICAL VAPOR DEPOSITION

Ayhan, Umut Barış
M.S., Department of Chemical Engineering
Supervisor: Prof. Dr. Güngör Gündüz
Co-Supervisor: Assoc. Prof. Dr. Burhanettin Çiçek

July 2004, 75 pages

Carbon nanotubes, which is one of the most attractive research subject for scientists, was synthesized by two different methods: Chemical vapor deposition (CVD), a known method for nanotube growth, and electron beam (e-beam), a new method which was used for the first time for the catalytic growth of carbon nanotubes.

In both of the methods, iron catalyst coated silica substrates were used for the carbon nanotube growth, that were prepared by the Sol-Gel technique using aqueous solution of Iron (III) nitrate and tetraethoxysilane. The catalytic substrates were then calcined at 450 °C under vacuum and iron was reduced at 500°C under a flow of nitrogen and hydrogen.

In CVD method the decomposition of acetylene gas was achieved at 600 °C and 750 °C and the carbon was deposited on the iron catalysts for nanotube growth. However, in e-beam method the decomposition of

acetylene was achieved by applying pulsed high voltage on the gas and the carbon deposition on the silica substrate were done.

The samples from both of the methods were characterized using transmission electron microscopy (TEM) and Raman spectroscopy techniques. TEM images and Raman spectra of the samples show that carbon nanotube growth has been achieved in both of the method. In TEM characterization, all nanotubes were found to be multi-walled carbon nanotubes (MWNT) and no single-walled carbon nanotubes (SWNT) were pictured. However, the Raman spectra show that there are also SWNTs in some of the samples.

Keywords: Carbon Nanotube, Chemical Vapor Deposition (CVD), Electron Beam (e-beam), Nanotechnology.

ÖZ

KİMYASAL BUHAR ÇÖKELTME YÖNTEMİ İLE KARBON NANOTÜP ÜRETİMİ

Ayhan, Umut Barış
Yüksek Lisans, Kimya Mühendisliği Bölümü
Danışman: Prof. Dr. Güngör Gündüz
Yardımcı Danışman: Doç. Dr. Burhanettin Çiçek

Temmuz 2004, 75 sayfa

Bu çalışmada, bilim dünyasının da en çok ilgisini çeken araştırma konularından biri olan karbon nanotüpler iki ayrı yöntem kullanılarak üretilmiştir. Bu yöntemler, (i) nanotüp üretiminde daha önceden de kullanılmakta olan 'Kimyasal Buhar Çökeltme' ve (ii) daha önce nanotüp üretiminde hiç kullanılmayan 'Elektron Demeti' yöntemidir.

Her iki yöntemde de nanotüpü elde edebilmek için katalizör olarak nanodemir kullanılmıştır. Nanodemir tanecikleri demir (III) nitrat ve tetra-etoksisilan karışımı çözeltinin kuvars cam üzerine sürülüp önce 450 °C de vakum altında kavrularak sonra da 500 °C de 'nitrojen + hidrojen' altında indirgenmesi yapılarak elde edilmiştir.

Kimyasal buhar çökeltme yönteminde asetilen gazı 600°C'de ve 750 °C'de ayrıştırılarak karbonun demir üzerine çökmesi sağlanmıştır. Elektron

demeti yönteminde ise ayrıştırma işlemi gaza darbeli yüksek voltaj uygulanarak yapılmış ve karbonun kuvars üzerine çökmesi sağlanmıştır.

İki sistemden de alınan örnekler ‘Geçirmeli Elektron Mikroskopu (TEM)’ ve ‘Raman Spektroskopi’ yöntemleri ile incelenmiştir. TEM resimleri ve Raman spektroskopi sonuçları örneklerde karbon nanotüp üretiminin başarıldığını göstermektedir. TEM resimlerinde görülen nanotüplerin hepsinin çok duvarlı nanotüpler olmasına karşın Raman spektroskopi sonuçları tekduvarlı karbon nanotüplerin varlığını da ortaya koymaktatır.

Anahtar Sözcükler: Karbon Nanotüp, Kimyasal Buhar Çökeltme, Elektron Demeti, Nanoteknoloji.

To My Family
&
İpek

ACKNOWLEDGEMENTS

First of all, I would like to express my deepest appreciation to my supervisor Prof. Dr. Güngör Gündüz for his valuable guidance, his humanity, his kindly attitude toward me and for sharing his knowledge in different areas apart from this subject matter throughout this study.

I would also like to thank my co-supervisor Assoc. Prof. Dr. Burhanettin Çiçek, Haydar Dişbudak, Hilal Göktaş for their suggestions and help, and Prof. Dr. Işık Önal for always being supportive, understanding and ready to help. Furthermore, I would like to thank Merih Şengönül and Assoc. Prof. Dr. Mehmet Somer for their help in the characterization of samples.

I would like to present my greatest thanks to my family, my brother in law Christopher Orr and especially to Nursel İpek Özmen for their continuous support, encouragement, trust and sacrifices for me that made the accomplishment of this work.

I wish to thank Berker Fıçıcılar and Burak Mutlu for not leaving me alone from the start of my university life, Misket Heper, Mustafa Onur Diri, Alper Uzun, Nezih Ural Yağşi, Sinan Ok, for their help, friendship and motivation during the hard course of this study. Special thanks to Özgür Kınacı for his extra motivation on this subject matter. Last but not least, I would like to thank my lab partners Evrim Şen, Ceylan Karakaya, Erhan Bat for their support and friendship, and many others that I could not mention here.

TABLE OF CONTENTS

LIST OF TABLES

Table

LIST OF FIGURES

Figure

NOMENCLATURE

A	Ampere
a_1, a_2	Unit vectors
C	Celsius
C_h	Chiral vector
cm	Centimeter
GHz	Giga Hertz
GPa	Giga Pascal
in	Inch
k	Thousand
K	Kelvin
kHz	Kilohertz
MPa	Mega Pascal
nm	Nanometer
T	Translation vector
THz	Tera Hertz
TPa	Tera Pascal
µm	Micron
θ	Chiral angle
Ψ	Rotation angle
τ	Translation
AFM	Atomic Force Microscope
CNT	Carbon Nanotube
CPU	Central Processing Unit
CVD	Chemical Vapor Deposition
DWNT	Double-Walled Carbon Nanotube

e-beam	Electron Beam
HRTEM	High Resolution Transmission Electron Microscope
ITO	Indium Tin Oxide
LCD	Liquid Crystal Display
MWNT	Multi-Walled Carbon Nanotube
RBM	Radial Breathing Mode
SWNT	Single-Walled Carbon Nanotube
SEM	Scanning Electron Microscope
STM	Scanning Tunneling Microscope
TEM	Transmission Electron Microscope
TFT	Thin Film Transistor
US	United States

CHAPTER 1

INTRODUCTION

Especially in the second half of the 20th century, the development in science and technology accelerated. New materials, like polymers, ceramics, etc., gave birth to new machines that make life easier. However, machines are usually huge in size when they are first invented. For example, the first computing machines (computers) were very huge in size that they were filling rooms. These devices were very useful but the big size of them was the major problem in their use in different areas or places.

Miniaturization is not, of course, a new idea. One of the most important and consistent aims of innovation has been to make things as small as possible, since smallness saves space and increases the mobility of devices. It brings probability, the possibility of putting more components together in order to achieve more sophisticated results and a saving in materials used and thus in cost. *Richard Feynman*, one of the 20th century's most famous and eclectic physicist, was who raised the idea that miniaturization might go all the way down to the molecular level, and that devices with components made from defined and countable numbers of atoms might be made. However, this was nothing more than a dream in the late 1950's, but this vision provoke the interest of ***Eric Drexler*** that made him go to the Massachusetts Institute of Technology in late 1970's and turning then into a PhD thesis and a book called "*Engines of Creation*", which was published in 1986. This was a revolutionary vision in manufacturing technology. Instead of being constructed from the top down, by moulding and machining big things into small ones, objects would be built from the bottom

up, from their constituent atoms. However, as a matter of fact, such constructions could not be done by the known processes of chemistry. Chemical processes involve reactions in solutions, liquid or gas. Instead, Dr. Drexler imagined a world of “molecular assemblers” – molecule-sized machines that would take individual atoms and position them exactly where required in the device under construction. To distinguish this process from the “solution-phase” of traditional chemistry, he described his new chemistry as “*machine-phase*”. Following these ideas he thought a name for this new technology and created the name “***Nanotechnology***”. [1]

Drexler’s description of nanotechnology has been changed through the years and it is generally being used for the production of new nanometer-sized materials by chemical or physical processes. However, these new materials are very close to the molecular size and easier to be processed, that these materials can help nanotechnology take its original description by Dr. Eric Drexler.

Nanotechnology is advancing especially in material sciences and biotechnology. When material sciences are in concern researches in polymer sciences, like nanocomposites, and ceramic researches are the leading studies in nanotechnology.

As a result of researches in the material sciences for new materials, *“Buckminsterfullerene”* (C_{60}), a hollow, pure carbon material shaped like a perfect soccer ball was discovered in 1985 by Richard Smalley, Harry Kroto, and their co-workers [2]. Other than C_{60}, materials consisting of different numbers of carbon atoms called as a general name *Fullerenes*, or *nanoballs* were also discovered. C_{70}, C_{80} are some examples to other fullerenes. These materials were so extraordinary that they bring new visions to scientists and the discoverers were rewarded with a Nobel Prize in Chemistry in 1996.

In 1991 carbon, once more, surprised the world of materials science with nanometer sized hollow tubes. Sumio Iijima, while trying to produce large amounts of fullerenes by arc-discharge method, noticed that there were tiny tubes of carbon among the soot [3]. These tubes of carbon are called “*Carbon Nanotubes*”. The first observed carbon nanotubes (CNT) were

concentric tubes one in another like famous Russian dolls, called multi-walled carbon nanotubes (MWNT). Then single-walled carbon nanotubes (SWNT), which consists of a single graphene layer rolled around a center, were discovered.

CNTs attracted the attention of scientists all over the world, working in very different disciplines, with their extraordinary properties. They have tensile strength and Young's modulus values far beyond metals that SWNTs have the highest tensile strength value any known material measured. CNTs are the stiffest known fiber, with a measured Young's modulus of 1.4 TPa and a tensile strength well above 100 GPa (possibly higher). For comparison, the Young's modulus of high-strength steel is around 200 GPa, and its tensile strength is 1-2 GPa. When electrical properties are considered they can be either metallic conductors or semiconductors depending on their precise structure. Individual CNTs have been observed to conduct electrons ballistically. They are the most conductive fibers known. In addition their semiconducting properties are known to be far better than silicon. Before CNTs, diamond was the best thermal conductor known. However, CNTs have now been shown to have a thermal conductivity at least twice that of diamond, along their tube axis.

CNTs can be used to improve the properties of the materials like polymers and ceramics. Thermally and electrically conducting polymers and ceramics can be produced with CNTs. Also it is possible to produce better semiconducting devices like transistors which are the basic components of computer microchips and LCD-TFT monitors.

CNTs are generally produced by three methods: arc discharge, laser ablation, and chemical vapor deposition (CVD). Laser ablation is the method by which fullerenes were first produced, and arc discharge is the method by which the CNTs were first produced. In laser ablation and arc discharge methods graphite is vaporized by laser beams and electrical arcs respectively and the vapor is then condensed. CVD is used to produce CNTs from gas phase carbon sources like acetylene, methane, and other carbon containing gases. In all of the three methods catalysts are used for the

carbon deposition. However, in arc discharge method it is possible to produce CNTs without catalysts. CVD, which was experimented in this study, is the mostly preferred method by the researchers because it is possible produce aligned CNTs at relatively low temperatures, below 1000°C.

In this study a stable CVD setup for the catalytic production of CNTs was constructed. It was aimed to produce CNTs using iron catalysts, which is the mostly preferred one, by the decomposition of acetylene gas at temperatures at 600-800°C under 180-200 Torr. In addition to this method a new method was tried for CNT growth which has never been used before: Electron beam (e-beam) method. In the e-beam method acetylene gas was decomposed by applying a pulsed high voltage, and carbon was deposited on the silica plates coated with iron catalysts. CNTs produced by both of the methods were characterized by Transmission electron microscopy (TEM) and Raman spectroscopy.

CHAPTER 2

LITERATURE SURVEY

2.1 Carbon Materials

Carbon, as being one of the important elements, is the key element for variety of matter. It is an element that exists in various polymorphic forms. Pure carbon materials have always been attracted the world of science as well as the rest of the world. Although it is really hard to classify the pure carbon materials, graphite, one of the polymorphic forms, is sometimes classified as a ceramic, and, in addition, the crystal structure of diamond, another polymorph, is similar to that of zinc blende.

2.1.1 Diamond

Diamond, being an attractive material by its beauty and properties, is a metastable carbon polymorph at room temperature and atmospheric pressure. Its crystal structure is a variant of the zinc blende, which is appropriately called the diamond cubic crystal structure. (figure 2.1.) The physical properties of diamond make it an extremely attractive material. It is extremely hard (the hardest known material), has a very low electrical conductivity, and before CNTs they were known to be the best thermal conductors; these characteristics are due to its crystal structure and the strong interatomic covalent bonds.

Diamond attracts the scientists with its physical and mechanical properties that can be helpful in many research areas. Through out the last decade diamond in the form of thin films has been produced. Film growth

technique involves vapor-phase chemical reactions followed by the film deposition.

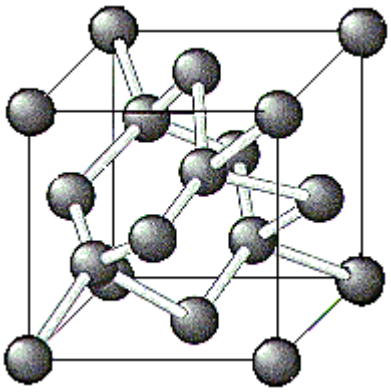

Figure 2.1 Unit cell of diamond that is one of the carbon polymorph**.**

The diamond is polycrystalline and may consist of very small and/or relatively large grains; in addition, amorphous carbon and graphite may be present. The mechanical, electrical, and optical properties of diamond films approach those of the bulk diamond material. These desirable properties have been and will continue to be exploited so as to create new and better products. For example, the surfaces of drills, dies, bearing surfaces, knives, and other tools have been coated with diamond films to increase surface hardness; some lenses and radomes have been made stronger while remaining transparent by the application of diamond coatings; coatings have also been applied to loudspeaker tweeters. Potential applications for these films include application to the surface of machine components such as gears and bearings, to optical recording heads and disks, and as substrates for semiconductor devices. [4]

2.1.2 Graphite

Another polymorph of carbon is graphite; it has a crystal structure distinctly different from that of diamond and is also more stable than diamond at ambient temperature and pressure. The graphite structure is composed of layers of hexagonally arranged carbon atoms; within the layers, each carbon atom is bonded to three coplanar neighbor atoms by strong covalent bonds.

(Figure 2.2) The fourth bonding electron participates in a weak van der Waals type of bond between the layers. As a consequence of these weak interplanar bonds, interplanar cleavage is facile, which results in the excellent lubricative properties of graphite. Furthermore, the electrical conductivity is relatively high in crystallographic directions parallel to the hexagonal sheets. High strength and good chemical stability at elevated temperatures, high thermal conductivity, low coefficient of thermal expansion and high resistance to thermal shock, high adsorption of gases, and good machinability are some other desirable properties of graphite.

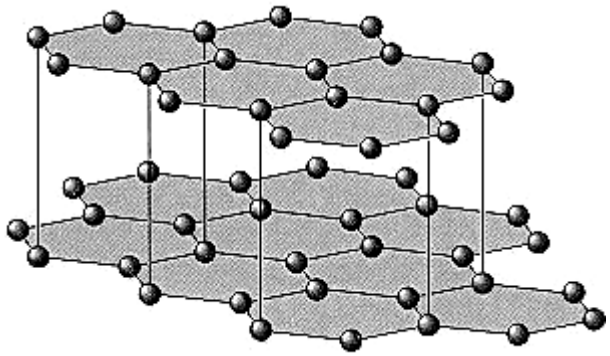

Figure 2.2 Structure of graphite.

Graphite is commonly used as heating elements for electric furnaces, as electrodes for arc welding, in metallurgical crucibles, in casting molds for metal alloys and ceramics, for high-temperature refractories and insulations, in rocket nozzles, in chemical reactor vessels, for electrical contacts, brushes and resistors, as electrodes in batteries, and in air purification devices. [4]

2.1.3 Fullerene

As being a newly discovered material, in 1985 [2], fullerenes are also another polymorphic form of carbon. Discovery of this material has shown that carbon is capable of forming extraordinary structures even out of reach of scientists can imagine. It exists in discrete molecular form, and consists of a hollow spherical cluster of sixty carbon atoms; a single molecule is denoted by C_{60}. Each molecule is composed of groups of carbon atoms that are

bonded to one another to form both hexagon (six-carbon atom) and pentagon (five-carbon atom) geometrical configurations. (figure 2.3.) One such molecule is found to consist of 20 hexagons and 12 pentagons, which are arrayed such that no two pentagons share a common side; the molecular surface thus exhibits the symmetry of a soccer ball. The material composed of C_{60} molecule. The structure of a C_{60} molecule is known as *Buckminster-fullerene,* named in honor of R. Buckminster Fuller, who invented the geo-desic dome; each C_{60} is simply a molecular replica of such a dome, which is often referred to as "buckyball" for short. The term *fullerene* is used to denote the class of materials that are composed of this type of molecule. [4]

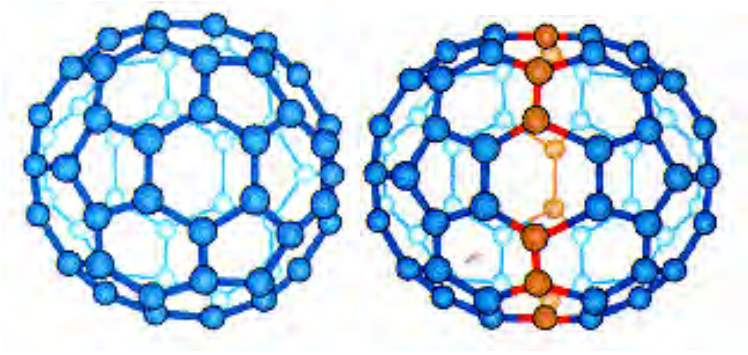

(a) **(b)**

Figure 2.3 (a) Buckminsterfullerene (C_{60}) molecule, (b) C_{70} molecule.

2.2 Carbon Nanotubes

2.2.1 Discovery

Very small diameter (less than 10 nm) carbon filaments were prepared in the 1970's and 1980's through the synthesis of vapor grown fibers by the decomposition of hydrocarbons at high temperatures in the presence of transition metal catalyst particles of <10 nm diameter. However, no detailed systematic studies of such very thin filaments were reported in these early years.

In 1985, C_{60} (buckminsterfullerene) molecule was discovered by Harry Kroto of the University of Sussex in England and a team at Rice University, Texas, led by Richard Smalley while experimenting a laser ablation system for the vaporization of graphite by laser beams and depositing them on a copper collector [2]. That carbon atoms could combine spontaneously into this complicated structure was astonishing, and the new perspectives that it opened up were acknowledged by the award of the 1996 Nobel Prize in chemistry to Smalley, Kroto and colleague Robert Curl. But until 1990, no one could make enough of it to study it properly or do anything useful with it and by that time researchers at Heidelberg in Germany and Tucson in the USA reported a method for making large quantities of the C_{60} molecule called arc discharge method [5].

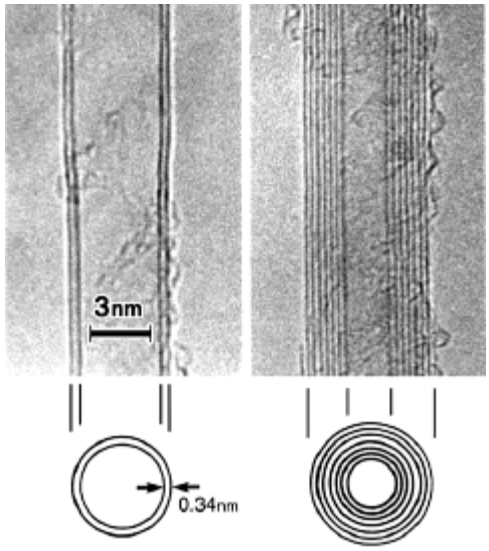

Figure 2.4 High Resolution Transmission Electron Microscope (HRTEM) image of first observed MWNTs by Iijima in 1991 [3].

In 1991 Iijima experimented with the arc discharge technique that had enabled the C_{60} researchers to make their new form of carbon in large quantities. By passing electrical sparks between two closely spaced graphite rods, Iijima vaporized them and allowed the carbon to condense in a sooty

mass. But when he looked at the soot through the microscope, he found something altogether unexpected. Amongst the debris, where others had found C_{60}, were tiny tubes of pure carbon, just a few nanometers across. These 'nanotubes' were hollow but many-layered: tubes inside tubes, like nested Russian dolls (figure 2.4 - 2.5), their ends sealed with conical caps [3]. These CNTs are called *multi-walled carbon nanotubes (MWNT)*.

Later on, in 1993, nearly at the same time Bethune et al. [6] and Iijima et al. [7] reported that *single-walled carbon nanotubes (SWNT)* (figure 2.6) have been produced using metal catalysts (Co) in an arc discharge system. In 1999 Iijima et al. reported a new kind of SWNT called *Nanohorn* that is SWNT with conical tube ends (figure 2.7) [8].

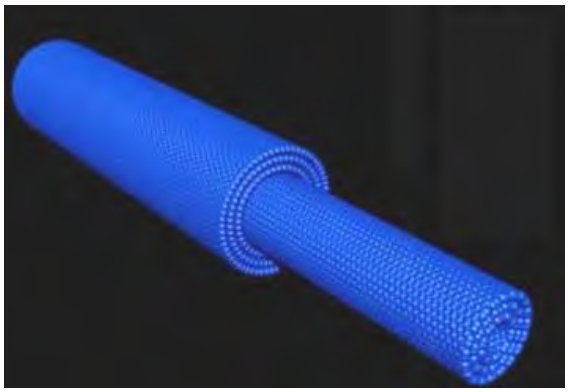

Figure 2.5 Computer generated image of a multi-walled carbon nanotube (MWNT).

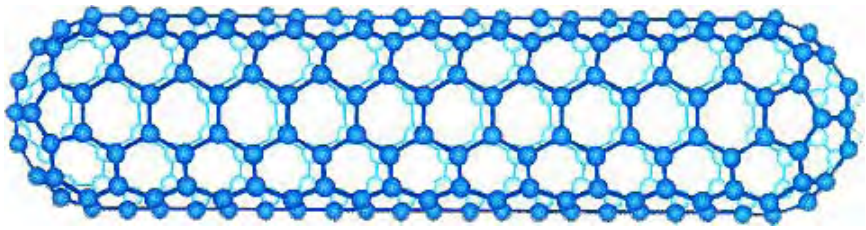

Figure 2.6 Computer generated image of a single-walled carbon nanotube.

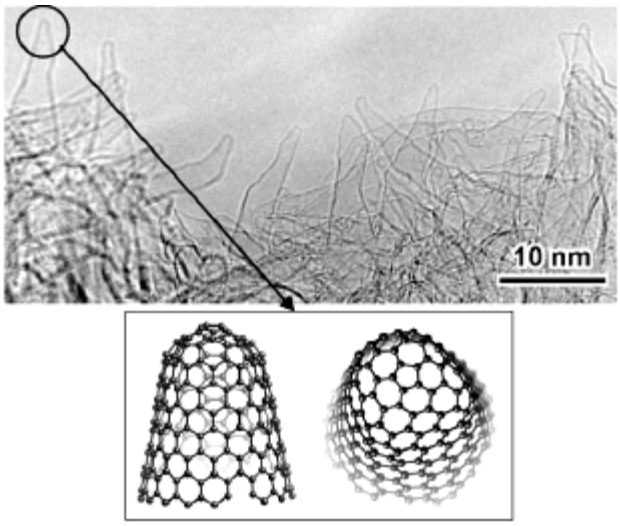

Figure 2.7 HRTEM (top) [8] and computer generated (bottom) images of single-walled carbon nanotubes [9].

2.2.2 Structure

The simplest way to imagine the structure of carbon nanotubes is to consider the conformal mapping of a finite number of two-dimensional layers of graphite sheet (graphene layers) onto themselves. Generally two distinct types of nanotubes exist, depending on whether the tube walls are made of one layer (graphene tubes) or more than one (graphitic tubes) [10]. The graphitic nanotubes known as multishell or multiwalled nanotubes consist of two or more concentric cylindrical shells of graphene sheets coaxially arranged around a central hollow, like Russian dolls, with a constant separation between the layers which is nearly equal to that of the graphite-layer spacing (0.34 nm; about 3–5% larger than single-crystal graphite spacing [9]). These have diameters ranging from 2 to 25 nm and lengths reaching up to several microns. The second kind consists of tubes made of single layers of graphene cylinders with a very narrow distribution in size range (0.7–2 nm) and lengths extending up to several microns. The interlayer correlations that give anisotropic physical properties to graphite is clearly absent in the single-wall nanotubes (they are also mostly absent in

multi-wall tubes due to rotational disorder between layers and topology but this is not so obvious) as isolated graphene layers make up the tubes. A single-wall nanotube can be considered in close analogy to a large fullerene molecule (closest is a C_{240} with a diameter of about 1.2 nm) which has been bisected, separated and joined with a tube 1 monolayer thick and having a similar diameter. However, both single and multi-wall nanotubes have the physical characteristics of solids, and must be seen as micro crystals and not as molecular species. They are reminiscent of typical chain polymerization reactions resulting in large molecular-weight structures but having different chain lengths. From a different point of view, carbon nanotubes are closely related to certain types of carbon fibers which have a similar cylindrical-layered structure but the former are far more perfect. As the single-wall nanotube contains all of the in-plane graphite strength, it can be thought of as the ultimate carbon fiber of molecular dimensions. [10]

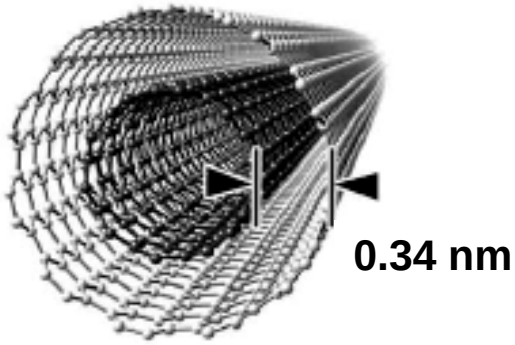

Figure 2.8 Distance between two nanotubes of a multi-wall carbon nanotube is nearly same as the interlayer distance of graphite. [8]

2.2.3 Classification of carbon nanotubes

The structure of CNTs has been explored by high resolution TEM and Scanning Tunneling Microscopy (STM) techniques (figure 2.9), yielding direct confirmation that the nanotubes are seamless cylinders derived from the

honeycomb lattice representing a single atomic layer of crystalline graphite, called a graphene sheet, (figure 2.10). Generally the diameter of a single-walled carbon nanotube about 0.7—10.0 nm, though most of the observed single-walled nanotubes have diameters less than 2 nm [11]. If the two ends of CNTs are neglected and focusing on the large aspect ratio of the cylinders (i.e., length/diameter which can be as large as 10^4-10^5), these nanotubes can be considered as one-dimensional nanostructures.

An interesting and essential fact about the structure of a carbon nanotube is the orientation of the six-membered carbon ring (hexagon) in the honeycomb lattice relative to the axis of the nanotube. Three examples of SWNTs are shown in figure 2.11. From this figure, it can be seen that the direction of the six-membered ring in the honeycomb lattice can be taken almost arbitrarily, without any distortion of the hexagons except for the distortion due to the curvature of the carbon nanotube. This fact provides many possible structures for carbon nanotubes, even though the basic shape of the carbon nanotube wall is a cylinder.

In figure 2.11, the terminations of each of the three nanotubes are shown. The terminations are often called caps or end caps and consist of a "hemisphere" of a fullerene. Each cap contains six pentagons and an appropriate number and placement of hexagons that are selected to fit perfectly to the long cylindrical section.

The primary symmetry classification of a carbon nanotube is as either being achiral (symmorphic) or chiral (non-symmorphic). An achiral carbon nanotube is defined by a carbon nanotube whose mirror image has an identical structure to the original one. There are only two cases of achiral nanotubes; armchair and zigzag nanotubes, as are shown in figure 2.11 (a) and (b), respectively. The names of armchair and zigzag arise from the shape of the cross-sectional ring, as is shown at the edge of the nanotubes in figure 2.11 (a) and (b), respectively. Chiral nanotubes exhibit a spiral symmetry whose mirror image cannot be superposed on to the original one. This tube is called a chiral nanotube, since such structures are called axially chiral in the chemical nomenclature [11].

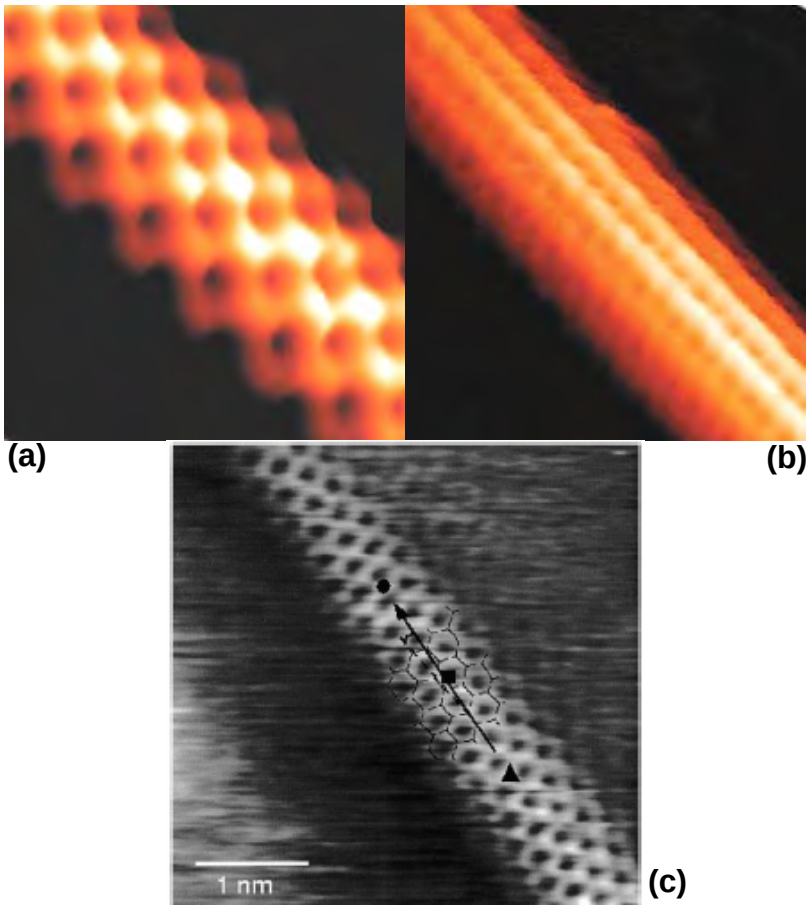

Figure 2.9 STM images of carbon nanotubes (a), (c) zigzag [12], and (b) armchair.

The structure of a SWNT is conveniently explained in terms of its 1D unit cell, defined by the vectors C_h and T in figure 2.10 (a).

The circumference of any carbon nanotube is expressed in terms of the chiral vector $C_h = n\mathbf{a_1} + m\mathbf{a_2}$ which connect two crystallographically equivalent sites on a 2D graphene sheet (Figure. 2.10 (a)). The construction in Figure 2.10 (a) depends uniquely on the pair of integers *(n, m)* which specify the chiral vector. Figure 2.10 (a) shows the chiral angle θ between the chiral vector C_h and the "zigzag" direction ($\theta = 0$) and the unit vectors $\mathbf{a_1}$ and $\mathbf{a_2}$ of the hexagonal honeycomb lattice of the graphene sheet.

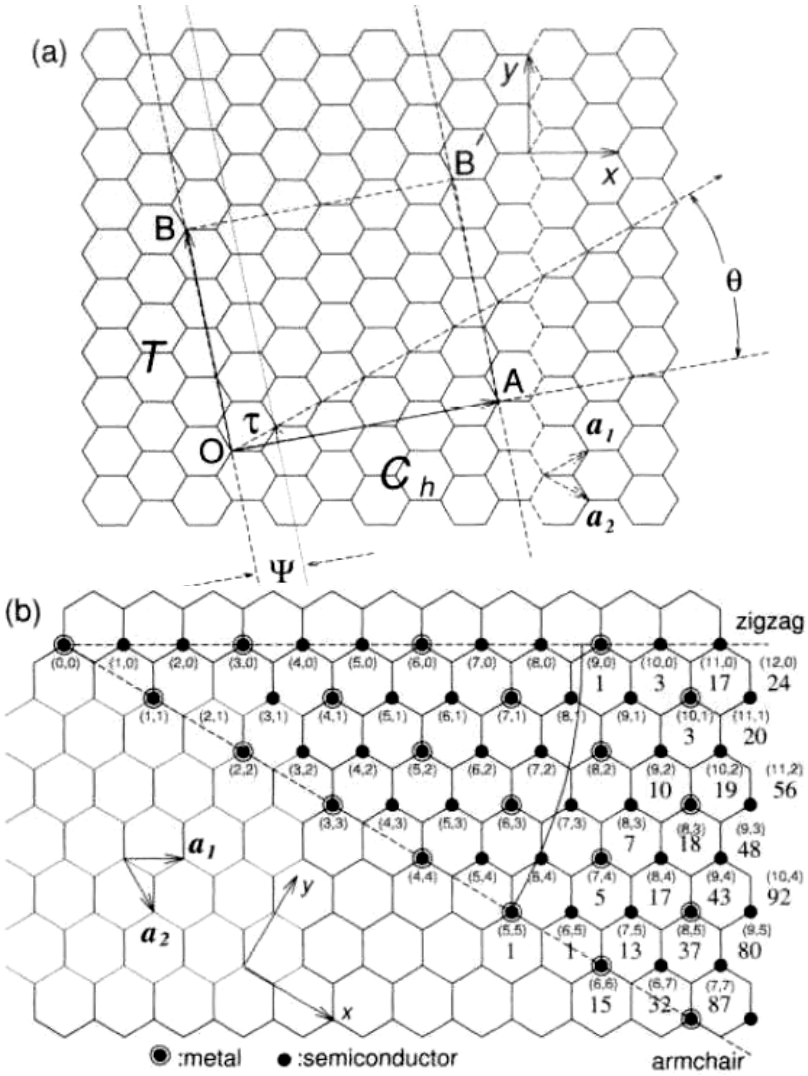

Figure 2.10 (a) The chiral vector $\overrightarrow{OA}$ or $C_h = na_1 + ma_2$ is defined on the honeycomb lattice of carbon atoms by unit vectors a_1 and a_2 and the chiral angle θ *with* respect to the zigzag axis. Along the zigzag axis $\theta = 0°$. Also shown are the lattice vector $\overrightarrow{OB} = T$ of the 1D nanotube unit cell and the rotation angle ψ and the translation τ which constitute the basic symmetry operation $R = (\psi \mid \tau)$ for the carbon nanotube. The diagram is constructed for (n, m) = (4, 2). **(b)** Possible vectors specified by the pairs of integers (n, m) for general carbon nanotubes, including zigzag, armchair, and chiral nanotubes. Below each pair of integers (n, m) is listed the number of distinct caps that can be joined continuously to the carbon nanotube denoted by (n, m). The encircled dots denote metallic nanotubes while the small dots are for semiconducting nanotubes. [10]

Three distinct types of nanotube structures can be generated by rolling up the graphene sheet into a cylinder as described below and shown in Figure 2.11. The zigzag and armchair nanotubes, respectively, correspond to chiral angles of $\theta = 0$ and 30°, and chiral nanotubes correspond to $0 < \theta < 30°$. The intersection of the vector $\overrightarrow{OB}$ (which is normal to C_h) with the first lattice point determines the fundamental one-dimensional (1D) translation vector T. The unit cell of the 1D lattice is the rectangle denned by the vectors C_h and T (Figure 2.10 (a)). [10]

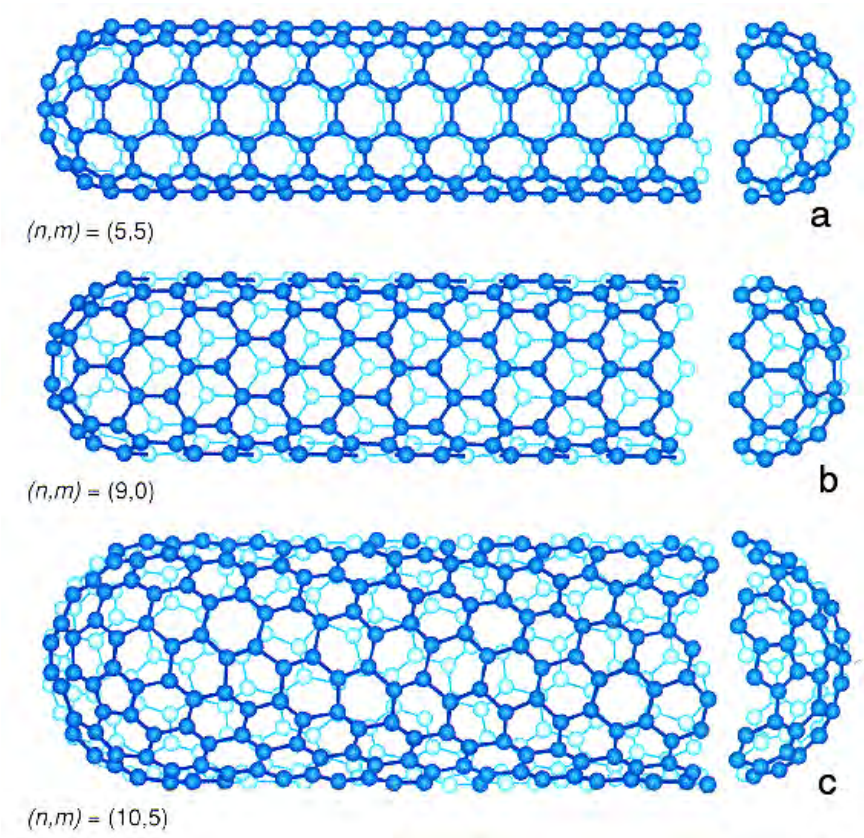

Figure 2.11 Classification of carbon nanotubes: **(a)** armchair, **(b)** zigzag, and **(c)** chiral nanotubes. From the figure it can be seen that the orientation of the six-membered ring in the honeycomb lattice relative to the axis of the nanotube can be taken almost arbitrarily.

2.2.4 Nanotube Growth Methods

2.2.4.1 Arc Discharge and Laser Ablation

Arc-discharge and laser ablation methods for the growth of nanotubes have been actively pursued in the past fifteen years. These methods are also being used for the production of fullerenes. Both methods involve the condensation of carbon atoms generated from evaporation of solid carbon sources. The temperatures involved in these methods are close to the melting temperature of graphite, 3000-4000°C. In laser ablation temperature can rise up to 10000°C.

In arc-discharge (figure 2.12), carbon atoms are evaporated by plasma of helium gas ignited by high currents passed through opposing carbon anode and cathode. Arc-discharge has been developed into an excellent method for producing both high quality multi-walled nanotubes and single-walled nanotubes. MWNTs can be obtained by controlling the growth conditions such as the pressure of inert gas in the discharge chamber and the arcing current. In 1992, a breakthrough in MWNT growth by arc-discharge was first made by Ebbesen and Ajayan who achieved growth and purification of high quality MWNTs at the gram level [13]. The synthesized MWNTs have lengths on the order of ten microns and diameters in the range of 5-30 nm. The nanotubes are typically bound together by strong van der Waals interactions and form tight bundles. MWNTs produced by arc-discharge are very straight, indicative of their high crystallinity. For as grown materials, there are few defects such as pentagons or heptagons existing on the sidewalls of the nanotubes. The by-products of the arc-discharge growth process are multi-layered graphitic particles in polyhedron shapes. Purification of MWNTs can be achieved by heating as grown material in an oxygen environment to oxidize away the graphitic particles. The polyhedron graphitic particles exhibit higher oxidation rate than MWNTs; nevertheless, the oxidation purification process also removes an appreciable amount of nanotubes.

For the growth of single-walled nanotubes, a metal catalyst is needed in the arc-discharge system. The first success in producing substantial amounts of SWNTs by arc-discharge was achieved by Bethune and coworkers in 1993. They used a carbon anode containing a small percentage of cobalt catalyst in the discharge experiment, and found abundant SWNTs generated in the soot material [6]. Nearly at the same time Iijima et al. also reported the growth of SWNTs in an arc discharge method using metal catalysts [7]. The growth of high quality SWNTs at the 1-10g scale was achieved by Smalley and coworkers using a laser ablation (laser oven) method. In 1996, a method was introduced for the production of carbon nanotubes called the laser ablation method (figure 2.13) [14]. The method utilized intense laser pulses to ablate a carbon target containing 0.5 atomic percent of nickel and cobalt. The target was placed in a tube-furnace heated to 1200°C. During laser ablation, a flow of inert gas was passed through the growth chamber to carry the grown nanotubes downstream to be collected on a cold finger. The produced SWNTs are mostly in the form of ropes consisting of tens of individual nanotubes close-packed into hexagonal forms via van der Waals interactions. The optimization of SWNT growth by arc-discharge was achieved by Journet and coworkers using a carbon anode containing 1.0 atomic percentage of yttrium and 4.2 atomic % of nickel as catalyst.

In SWNT growth by arc-discharge and laser ablation, typical by-products include fullerenes, graphitic polyhedrons with enclosed metal particles, and amorphous carbon in the form of particles or overcoating on the sidewalls of nanotubes. A purification process for SWNT materials has been developed by Smalley and coworkers and is now widely used by many researchers. The method involves refluxing the as-grown SWNTs in a nitric acid solution for an extended period of time, oxidizing away amorphous carbon species and removing some of the metal catalyst species.

The success in producing high quality SWNT materials by laser-ablation and arc-discharge has led to wide availability of samples useful for

studying fundamental physics in low dimensional materials and exploring their applications. [10]

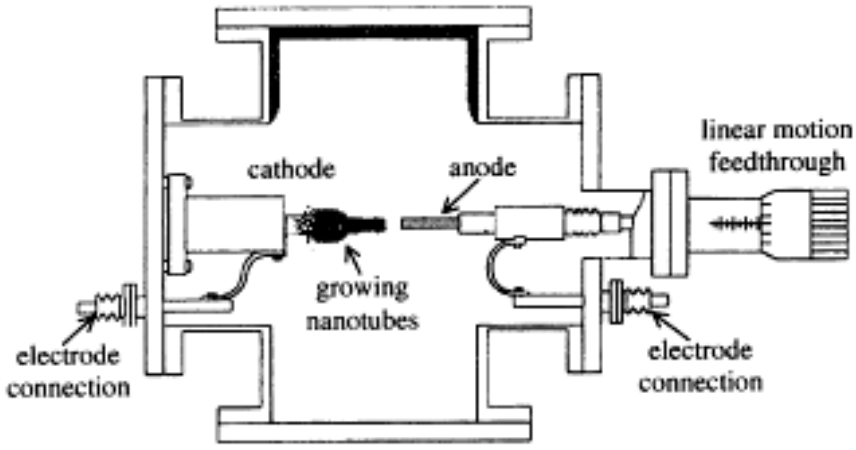

Figure 2.12 Experimental setup of arc discharge method for CNT and fullerene production [11].

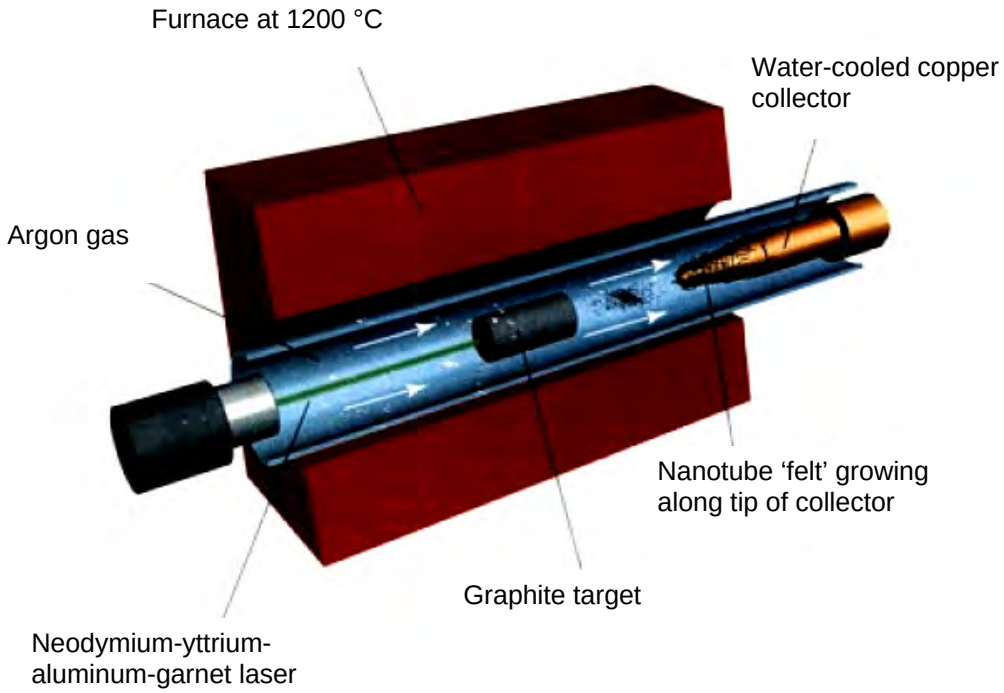

Figure 2.13 Schematic representation of laser ablation set-up [11].

2.2.4.2 Chemical Vapor Deposition (CVD)

Chemical vapor deposition (CVD) method (figure 2.14) has been used for at least 4 decades for the production of carbon filaments, which is based on the decomposition of carbon-containing gases on metal catalysts at reaction temperatures below 1000°C that is far below the temperatures involved in the arc discharge and laser ablation methods [15].

The growth process involves heating a catalyst material to high temperatures in a tube furnace and passing a hydrocarbon gas through the tube reactor for a period of time. Materials grown over the catalyst are collected upon cooling the system to room temperature. The key parameters in nanotube CVD growth are the hydrocarbons, catalyst and growth temperature. The active catalytic species are typically transition-metal nanoparticles formed on a support material such as alumina. The general nanotube growth mechanism in a CVD process involves the dissociation of hydrocarbon molecules catalyzed by the transition metal, and dissolution and saturation of carbon atoms in the metal nanoparticles. The precipitation of carbon from the saturated metal particle leads to the formation of tubular carbon solids in sp^2 structure. Tubule formation is favored over other forms of carbon such as graphitic sheets with open edges. This is because a tube contains no dangling bonds and therefore is in a low energy form. MWNT growth, most of the CVD methods employ ethylene or acetylene as the carbon feedstock and the growth temperature is typically in the range of 550-900°C. Iron, nickel or cobalt nanoparticles are often used as the catalyst. The rationale for choosing these metals as catalyst for CVD growth of nanotubes lies in the phase diagrams for the metals and carbon. At high temperatures, carbon has finite solubility in these metals, which leads to the formation of metal-carbon solutions and therefore the aforementioned growth mechanism (figure 2.15). Noticeably, iron, cobalt and nickel are also the favored catalytic metals in laser ablation and arc-discharge. This simple fact may hint that the laser, discharge and CVD growth methods may share a

common nanotube growth mechanism, although very different approaches are used to provide carbon feedstock.

In 1996, Li et al. used sol-gel process for the preparation of mesoporous silica containing iron nanoparticles from tetraethoxysilane (TEOS) hydrolysis in iron nitrate aqueous solution following with calcination and reduction under a flow of H_2/N_2 mixture, and produced MWNT at 700 °C [17]. In 1999, Pan et al. also used the same method but with some modifications in the composition of solution for the sol-gel process, and carried the CNT growth at 600 °C which was 100 °C lower than the previous study [18]. In both of the studies acetylene (C_2H_2) was used as the carbon source.

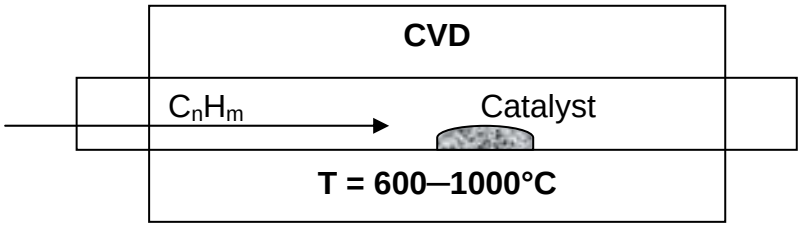

Figure 2.14 Schematic representation of experimental setup for nanotube growth by chemical vapor deposition.

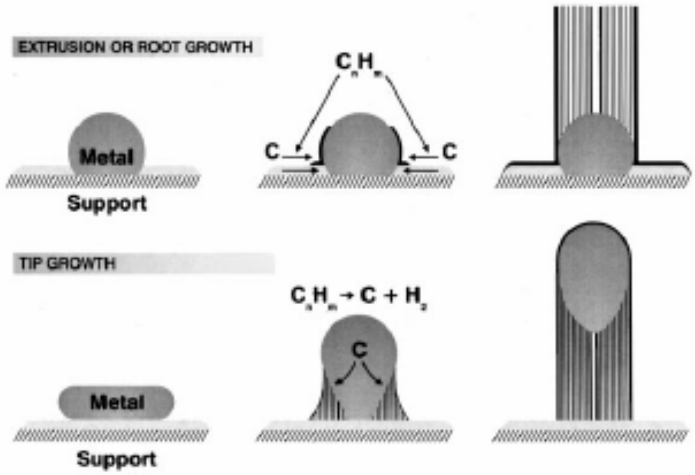

Figure 2.15 Schematics of tip-growth and extrusion mechanisms for carbon filament growth. [16]

In 2000, M. Su et al. introduced a new form of powder catalyst consisting of Fe, Mo, and Al, and produced high-quality SWNTs at about 850 – 1000 °C [19]. In 2001, Lee et al. achieved success in the production of CNTs on iron catalyst by a two-stage CVD process in which the gases first enter the 850 °C zone and then come to the 550 °C zone where the catalyst containing substrates are [20]. Another study was reported by Lee et al. in 2001 where the vertically aligned CNTs were grown on Fe-deposited on silica substrates using thermal CVD of acetylene gas at 950°C. In this study, the size of Fe particles was controlled by the flow rate of the NH_3 gas and pretreatment time, which was led to control the diameter of CNTs. The results are given in the Table 2.1 [21]. Emmenegger et al. in 2003 came with another study using again iron catalyst stating that the parameters like the time of deposition, the temperature and the iron nitrate concentration affects the CNT density, and furthermore they suggested some growth mechanisms for CNT growth [22].

Table 2.1 Average diameter and growth rate of CNTs depending on the system condition [21].

Number of experiments	NH_3		C_2H_2		Average Fe particle diameter (nm)	Average CNT diameter (nm)	CNT length (μm)	Growth rate (μm/min)
	Flow rate (sccm)	Time (mm)	Flow rate (sccm)	Time (mm)				
4	100	20	30	10	200	130	12	1.2
3	300	120	30	10	130	60	18	1.8
2	300	240	30	10	400	240	8	0.8
2	100	20	30	3	200	130	3.6	1.2
2	100	20	30	20	200	130	20	1
2	100	20	30	30	200	130	28	0.9

In all of the above studies iron was the catalyst and C_2H_2 gas was the carbon source for the CNT growth. However, in many other studies metals like Ni and Co were used as the catalyst and hydrocarbons like methane (CH_4) gas was used as the carbon source for the catalytic growth of CNTs by CVD.

Table 2.2 Summary of results of methane CVD experiments using supported metal-oxide catalysts [23].

Catalyst composition	Support material	SWNTs?	Description of synthesized material
Fe_2O_3	alumina	yes	abundant individual SWNTs; some bundles; occasional double-walled tubes
Fe_2O_3	silica	yes	abundant SWNT bundles
CoO	alumina	yes	some SWNT bundles and individual SWNTs
CoO	silica	no	no tubular materials synthesized
NiO	alumina	no	mainly defective multi-walled structures with partial metal filling
NiO	silica	no	no tubular materials synthesized
NiO/CoO	alumina	no	no tubular materials synthesized
NiO/CoO	silica	yes	some SWNT bundles

Kong et al., in 1998, produced of SWNTs using silica and alumina supported Fe_2O_3 catalyst using methane as the carbon source. They also produced SWNTs and MWNTs at 1000°C by using different metal catalysts as shown in the Table 2.2 [23]. This study was then followed by another study by Mukhopadhyay et al. in which acetylene was deposited on different metal catalysts supported by Y-type zeolite, alumina, and silica where the results are show in Table 2.3 [24]. In addition to these Lee et al. in 2001 investigated the effect of temperature on the growth of CNTs and concluded that the growth rate, the diameter, the density, and the structure of CNTs could be controlled by adjusting the growth temperature [25]; then they compared the catalyst effect on CNTs synthesized by thermal CVD using silica supported Ni, Co, and Fe catalysts [26].

Li et al. have produced very uniform and clean double-walled carbon nanotubes (DWNT) from Co particles dispersed on porous MgO nanoparticles, with the decomposition of CH_4 at 1000°C in 2003 [27]. Nearly at the same time Hiraoka et al. have selectively synthesized DWNTs by using catalytic decomposition of C_2H_2 on well-dispersed Co/Fe binary catalysts supported on heat resistant zeolite at temperatures above 900°C and stated that below this temperature the majority of the nanotubes produced were SWNTs and MWNTs [28].

Table 2.3 Effect of reaction temperature, flow rate of the gases, support and metal particles on the quality and quantity of nanotubes [24]

Support	Metals used	Reaction time (min)	Temp. (°C)	Gas flow rate: N_2 flow; C_2H_2 flow (ml/min)	Comment
Y-type zeolite	Co–V	60	700	120; 15	high density and quasi aligned
Y-type zeolite	Co–V	60	600	120; 15	less dense but quasi aligned
Y-type zeolite	Co–V	30	700	120; 15	less dense but quasi aligned
Y-type zeolite	Co–V	45	700	120; 15	less dense but quasi aligned
Y-type zeolite	Co–V	60	700	200; 25	quasi aligned but not homogeneous in nature
Y-type zeolite	Co–V	60	700	85; 25	high amount of amorphous carbon
Y-type zeolite	Co–Fe	60	600	120; 15	high density and quasi aligned
Y-type zeolite	Co–Fe	60	700	120; 15	quasi aligned but high amount of amorphous carbon and also slightly thick nanotubes
Y-type zeolite	Co–Ni	60	700	120; 15	less dense and not aligned
Y-type zeolite	Co–Pt	60	700	120; 15	less dense and not aligned
Y-type zeolite	Co–Y	60	700	120; 15	less dense and not aligned
Y-type zeolite	Co–Cu	60	700	120; 15	not active, almost no nanotubes
Y-type zeolite	Co–Sn	60	700	120; 15	not at all active
Commercial grade alumina	Co–V	60	700	120; 15	high density and quasi aligned
Commercial grade silica	Co–V	60	700	120; 15	high density but not aligned

2.2.5 Characterization

When nano-materials are in concern, characterization becomes to be the most difficult subject, and when carbon nanotubes are in concern transmission electron microscopy (TEM), scanning electron microscopy (SEM), and Raman spectroscopy are the generally used methods for the characterization.

In SEM characterization it is possible to see the orientation of the CNTs on the surface without any pretreatment of the substrates since the CNTs are electrically conductive. However, in TEM characterization of CNTs the deposit are taken from the surface of the support material by some

suspensions like methanol, chloroform, etc. then the solution is drop-dried on the carbon film coated TEM grids [29]. By TEM characterization of the CNTs it is possible to have information about the structure and type of the CNTs as being SWNT or MWNT. TEM and SEM analysis had been the main characterization method in many of the researches (figure 2.3 and figure 2.4) [17-29].

In some of the studies atomic force microscopy (AFM) has also been used for the 3D images of CNTs (figure 2.16) [23]. However, it is not possible to have the images of very small CNTs with AFM. In addition scanning tunneling microscopy (STM) is an important method for the characterization of the atomic structure of CNTs (figure 2.9 (c)) [12].

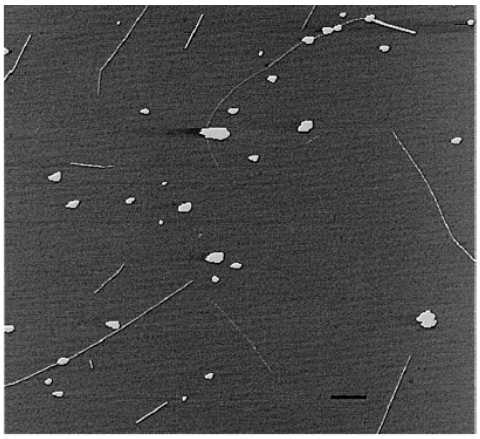

Figure 2.16 Tapping mode AFM image of carbon nanotubes produced on the Fe_2O_3/alumina catalyst. Z range dark to bright: 4 nm. Scale bar: 0.5 μm. Sonication may have caused some of the short nanotubes [23].

Apart from these microscopy techniques, Raman spectroscopy has been shown to be a powerful tool for characterizing SWNTs. The characteristic peaks occur due to the radial breathing mode (RBM), disordered carbon (D–band), and an out-of-phase graphene sheet-like vibrations (split G–band). These peaks occur at approximately 170 – 325, 1330, and 1585 nm, respectively. The radial breathing mode is present in SWNTs only. An asymmetry on the right side of the G–band represents the

peak characteristic of multi-wall carbon nanotubes (MWNTs), and occurs at 1620 nm. The peak at 1585 nm (primary G–peak) is due to longitudinal vibrations along the graphene sheet, and the peaks at 1567 and 1543 nm are due to transverse graphene sheet vibrations. The Raman spectroscopy signature of SWNTs is unique and can be used to identify the presence of the nanotubes [30]. It is one of the widely used characterization method for CNTs. Pimenta et al. in 1998 studied on the raman modes of metallic CNTs, produced by arc discharge method, with different laser energies in a range of 0.94 – 3.05 eV and found raman peaks at wavelengths in arrange of 1500 – 1600 nm (G–Band) showing the tangential modes and peak at wavelength 180 nm (RBM: Radial Breathing Mode) that is uniquely observed for the SWNTs and the intensity of the peaks at the RBM are strongly dependent on the energy of the laser used in the Raman spectroscopy [31]. Another study by Zhang et al. characterized the SWNTs produced by CO_2 continuous laser vaporization and found peaks nearly at the same wavelengths 189 nm RBM and 1538 and 1581 nm G–band [32]. In 2002, Dresselhaus et al. published their study about the Raman spectroscopy on the isolated SWNTs and reviewed the Raman spectroscopy of SWNTs. In the below Table 2.4 the vibrational modes observed for CNTs are given [33].

Table 2.4 Vibrational modes observed for Raman scattering in SWNTs.

Notation	Frequency (cm^{-1})	Symmetry	Type of mode
RBM[a]	248 /d_t	A	In phase radial displacements
D-band	~1350	–	Defect-induced, dispersive
G-band	1550–1605	A, E_1, E_2	Graphite-related optical mode[b]
G'-band	~2700	–	Overtone of D-band, highly dispersive

[a] RBM denotes radial breathing mode.
[b] The related 2D graphite mode has E_{2g} symmetry. In 3D graphite, the corresponding mode is denoted by E_{2g2}

Following these works Okazaki et al. characterized the SWNTs synthesized by hot-filament assisted CVD of various alcohols with Raman spectroscopy [34].

In 2001 Bandow et al. published a Raman scattering study of DWNTs derived from the chains of fullerenes in SWNTs [35] and in 2003 Wei et al. studied the Raman spectroscopy of the DWNTs [36].

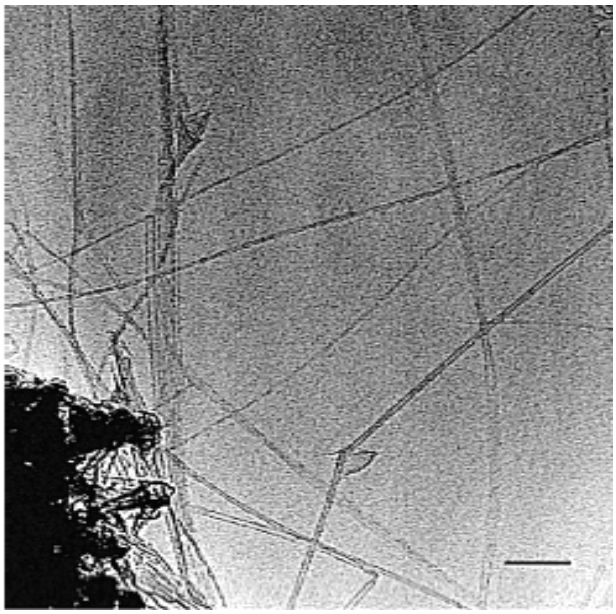

Figure 2.17 TEM image of individual and bundled SWNTs produced on the FeO alumina catalyst. Scale bar: 100 nm. [23]

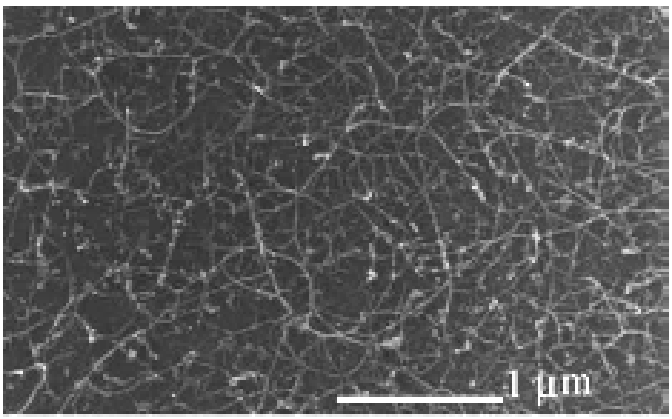

Figure 2.18 SEM images of 2-nm-thick Fe-coated sapphire substrates after methane CVD at 800 °C [29].

Furthermore, there appeared some recent works on the purification processes of CNTs. The purification processes are generally consisted of an acid refluxing for the removal of metal catalyst particles following with the oxidizing and annealing steps for the removal of other deposits like amorphous carbon [37-40]. In one of these purification studies by Strong et al. as with the details of the purification method, broad information about the characterization of SWNTs was also given [30].

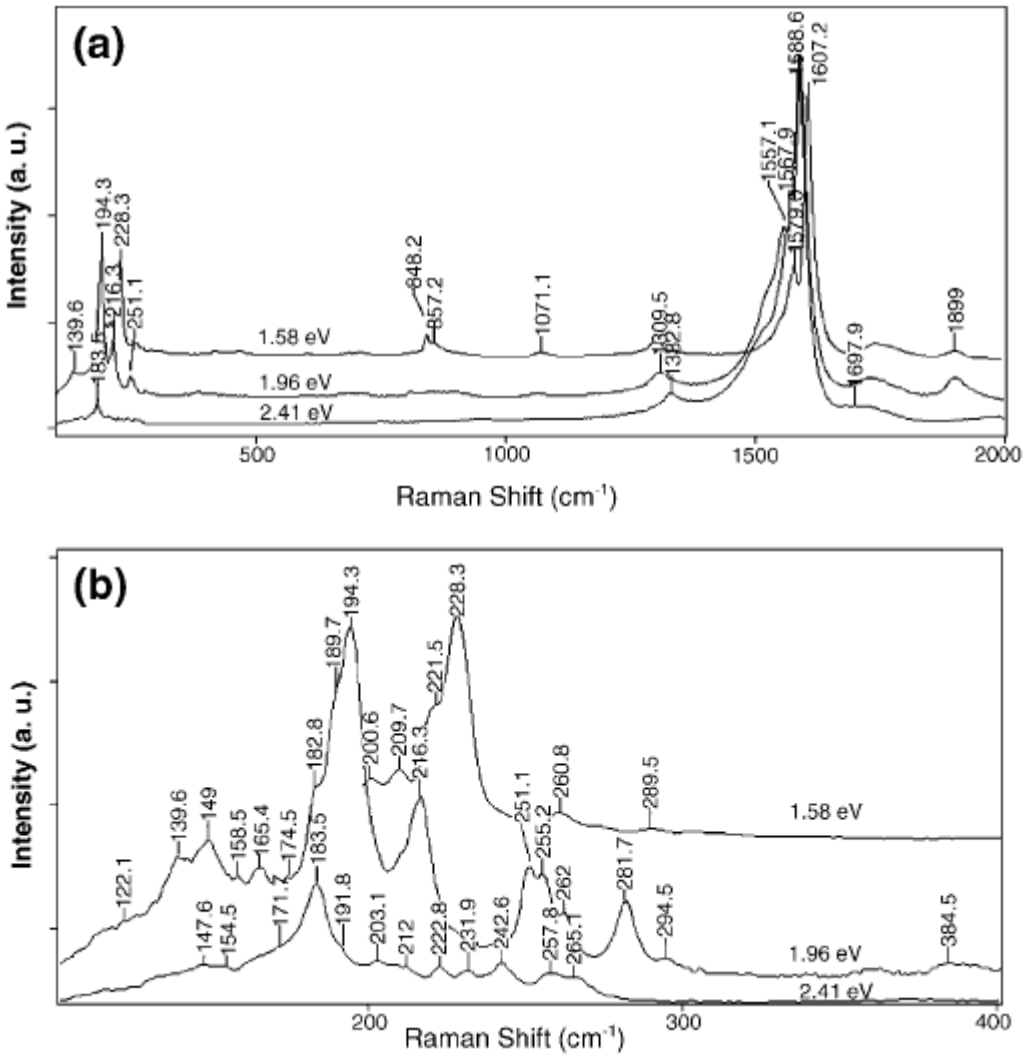

Figure 2.19 (a) Raman spectra of the CNTs at different E_{laser} excitation. **(b)** A close-up view of the RBM of the CNTs at different E_{laser} excitation. [36]

2.2.6 Properties

Because of their nanometer scale dimensions, the nanotubes can have novel properties and yield unusual scientific phenomena. However, most of the known properties of the nanotubes are theoretical but with the improvement of the characterization techniques it has been seen that the theoretical properties of the nanotubes do not differ very much from the experimental results.

These quasi-one-dimensional objects have highly unusual electronic properties. For the perfect tubes, theoretical studies have shown that the electronic properties of the carbon nanotubes are intimately connected to their structure. They can be metallic or semi-conducting, depending sensitively on tube diameter and chirality (helicity). Experimental studies using transport, scanning tunneling, and other techniques have basically confirmed the theoretical predictions. The electric responses of the carbon nanotubes are found to highly anisotropic in general. Ropes of CNTs were measured with a resistivity of 10^{-4} ohm-cm at 300 K [14], making them the most conductive fibers known. Individual tubes have been observed to conduct electrons ballistically, that is, with no scattering, with no coherence lengths of several microns [41]. In addition, they can carry the highest current density of any known material, measured as high as 109 A/cm^2 [42], and Phaedon Avouris, the director of IBM's Center for Nanoscale Science and Technology, has suggested that it could be as high as 1013 A/cm^2. Also CNTs, besides its superconducting properties, have extraordinary semi-conducting properties, that is, they have 20 times better transconductance compared with that of silicon transistors [43].

The heat capacity of single-walled nanotubes is predicted to have characteristic linear temperature dependence at low temperature [10]. Before CNTs diamond was the best thermal conductor known but CNTs have now been shown to have thermal conductivity at least twice that of diamond [44].

Carbon nanotubes have such mechanical properties that can not be underestimated. Although the carbon nanotubes were discovered in 1991 the

property studies could have only be started about year 1996. The mechanical properties, like Young's modulus and tensile strength, of carbon nanotubes show that they can replace metals in variety of applications. In 1996, Ebbesen et al. calculated Young's modulus values varying from 0.27 TPa to 4.15 TPa with an average of 1.8 TPa [47]. Following this in 1998 Treacy et al. calculated a Young's modulus value of 1.25 TPa [48]. Tensile strength values varying from 11 GPa to 63 GPa has been calculated by Yu et al. in 2000 [49], also Pantano et al. calculated Young's moduli values varying from 270 GPa to 950 GPa in 2004. [50]

Table 2.5 Thermal conductivities of several materials [45].

Materials	**Thermal Conductivity, k (W/m-K)**
Aluminum	237
Chromium	93.7
Copper	401
Gold	317
Iron	80.2
Stainless Steel AISI 302	15.1
Lead	35.3
Magnesium	156
Nickel	90.7
Platinum	71.6
Silver	429
Titanium	21.9
Tungsten	174
Silicon carbide	490
Graphite (parallel to layers)	1950
Diamond	2300
CNTs	**2000-11000** [46]

Table 2.6 Some typical tensile strengths of several materials [51].

Materials	Ultimate Strength (MPa)
Structural Steel ASTM-A36	400
Steel High strength alloy ASTM A-514	760
Stainless Steel AISI 302 - Cold-rolled	860
Cast Iron 4.5% C, ASTM A-48	170
Aluminum Alloy 2014-T6	455
Copper 99.9% Cu	220
Titanium Alloy (6% Al, 4% V)	900
Nylon, type 6/6	75
Rubber	15
Marble	15
SWNT	**6300**

Table 2.7 Approximate Young's moduli of various solids [51].

Materials	Young's modulus (E) (MPa)
Rubber (small strain)	6.9
Human tendon	551.6
Unreinforced plastics, polyethylene, nylon	1,379
Wood (along grain)	6,895
Fresh bone	20,685
Magnesium metal	41,370
Ordinary glasses	68,950
Aluminum alloys	68,950
Brasses and bronzes	117,215
Iron and steel	206,850
Aluminum oxide (sapphire)	413,700
Diamond	1,172,150
CNTs (average)	**2,000,000**

2.2.7 Applications

Although the properties of carbon nanotubes are not confirmed, and are still being investigated, with the known properties it is not too difficult to

think that carbon nanotubes can be used in many different applications. It is possible to say that carbon nanotubes will replace the materials in some applications and also they will create some new application areas.

With the increase in the number of the studies about the possible applications of the carbon nanotubes, it has been seen that they will speed up the development of technology.

Most of the recent studies on the applications of carbon nanotubes are on the production of new composite materials because of their incredible mechanical and electrical properties. According to some of the studies carbon nanotubes can be used to make polymers with better physical and mechanical properties [52], though US Army is investing money on the research for the new composite materials to be used in the production of more durable soldier uniforms.

Another application for carbon nanotubes is that they can be used in the production of transparent conductive coatings. Generally indium tin oxide (ITO) is used for such coatings. However these coatings give better results when produced from carbon nanotubes [53]. These coatings are being planned to be used to produce invisible vehicles by coating them and give the coating the image of the surroundings.

Table 2.8 Comparison of competitive transparent conductive coating technology [53].

	CNT dispersions	Sputtered ITO	ITO dispersions	Nano Metal dispersions
Transparency	☑	☑	●	●
Conductivity	●	☑	✘	☑
Cost	☑	●	☑	✘
Color	☑	●	✘	☑
Printing capability	☑	✘	●	✘
Flexibility / durability	☑	✘	✘	☑
Environmental stability	☑	☑	☑	☑

☑ Excellent ● Good ✘ Poor

The electrical properties of the carbon nanotubes show that they can be used in many applications in the electronics industry. It has been reported by IBM that the carbon nanotubes have shown more than ten times better semi-conducting performances than silicon. [54] Transistors produced from carbon nanotubes can be used in the microchips and LCD – TFT monitors. NEC Corporation has reported that they have developed a standardized method for the production of carbon nanotube transistors having better transconductance than that of silicon transistors [43]. According to a very recent study researchers have developed a single carbon nanotube transistor that is operating at 2.6 GHz so that in the future it is possible to have computer CPU's (Central Processing Unit) operating at speeds like THz [55].

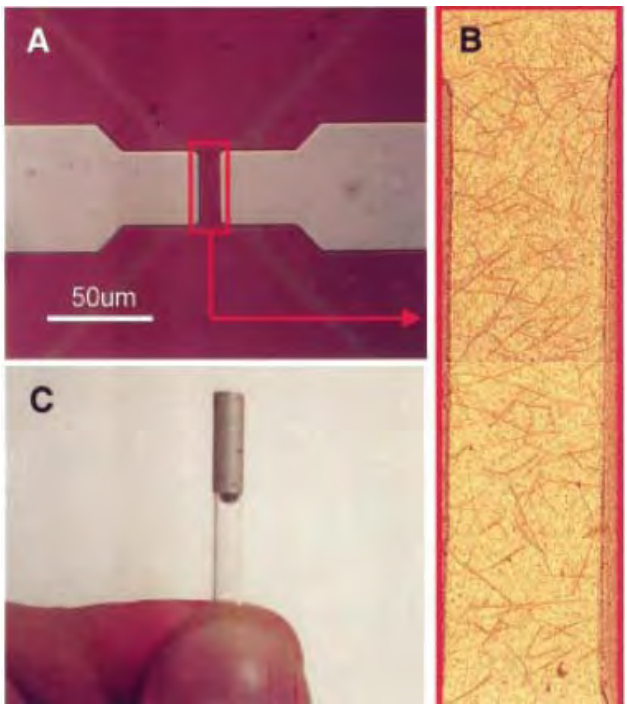

Figure 2.20 (a) Optical micrograph of a SWNT device. Ti contacts were evaporated on top of a SWNT film grown on thermal SiO_2. The source/drain channel dimensions are 10x30 μm^2. The Si substrate serves as a back gate. **(b)** Representative AFM image of a SWNT network that shows multiple conduction pathways via interconnected CNTs. **(c)** Optical micrograph of a SWNT flow-cell chemiresistor sensor made from ⅛ in. outer diameter quartz tubing. [57]

Carbon nanotubes are also used in the fuel cells as electrodes. These fuel cells have been constructed by the NEC Corporation and the results are very promising [56]. Researches have shown that CNTs have the highest reversible capacity of any carbon material for use in lithium-ion batteries [57]. In addition, CNTs are outstanding materials for super capacitor electrodes [58], and are now being marketed.

Furthermore carbon nanotubes can be used in the production of the nerve gas sensors, since the nanotubes react by an increase in their electrical resistance when exposed to nerve gases. [59]

Figure 2.21 Computer generated illustrations of space elevators [60].

These possible applications and extraordinary properties for the carbon nanotubes give courage to the researchers to find out new application areas for the nanotubes and it is possible to foresee that the carbon nanotubes will take an important place in the development of science and technology. A theory, first mentioned by futurologist and science fiction author Arthur C. Clark, about the ‘space elevators’ are now considered to be feasible after the physical and mechanical properties of CNTs are calculated. ‘Space elevators’ is a project about going to the space platforms on the orbits outside of the atmosphere by elevators made of CNTs [51, 60].

CHAPTER 3

EXPERIMENTAL

3.1 Catalyst Preparation

In the production of carbon nanotubes, catalysts play a distinct role since they are used to determine the type (single wall or multi wall) and the alignment of carbon nanotubes.

In our experiments, iron was chosen to be the catalyst since it is possible to produce both single wall and multi wall carbon nanotubes, and iron is an easy-to-find type of material.

In the preparation of the catalyst sol-gel method was used. This method was used in order to have a homogeneous distribution of catalyst particles on the surface on which carbon nanotubes would be grown. In this method:

(i) 7.5 ml of 1.5 M Iron (III) Nitrate solution

(ii) 5 ml of Tetraethoxysilane (TEOS)

(iii) 15 ml of Ethanol

were mixed for 20 minutes by a magnetic stirrer and then a few drops (~0.4 ml) of hydrofluoric acid (HF) were added to the mixture and was stirred for another ~25-30 minutes [18]. The solution was then drop dried on the previously prepared ~1 cm x 1 cm silica plates. The plates and the remaining solution were dried in the oven at about 100 °C overnight in order to remove the excess water on the catalysts. After drying the solution was made to be powder. The silica plates and the powder catalysts were then put on the sample holders and were introduced to the quartz tube furnace in the CVD setup.

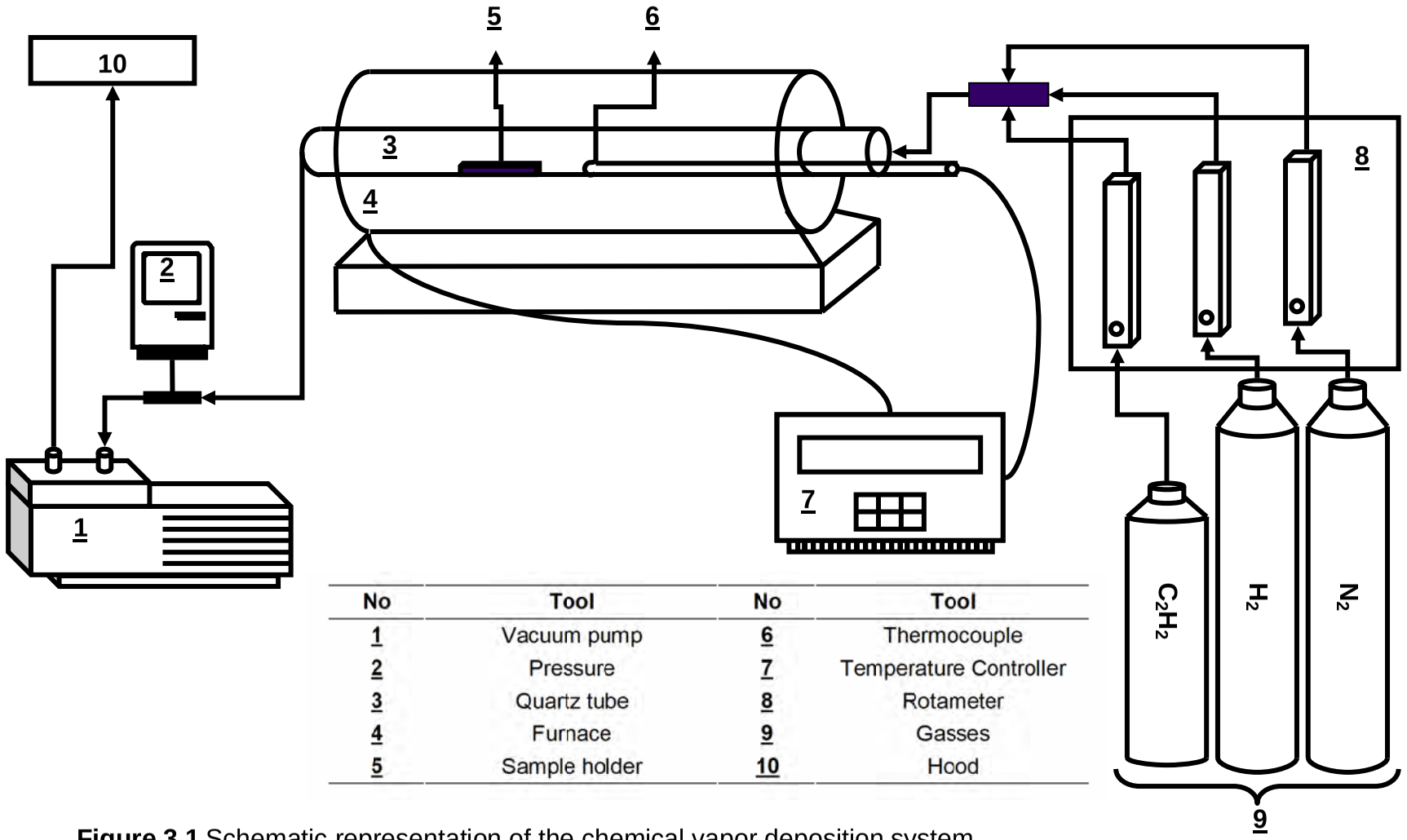

No	Tool	No	Tool
1	Vacuum pump	6	Thermocouple
2	Pressure	7	Temperature Controller
3	Quartz tube	8	Rotameter
4	Furnace	9	Gasses
5	Sample holder	10	Hood

Figure 3.1 Schematic representation of the chemical vapor deposition system.

The catalysts were calcined at 450 °C under vacuum (~10^{-3} Torr) for 10 hours in order to crack catalyst particles into smaller sized nanoparticles. Then the catalysts were reduced at 500 °C under ~180-200 Torr pressure in a flow of 10 % H_2 and 90 % N_2 for 5 hours.

3.2 Chemical Vapor Deposition (CVD) Method

After the catalysts were prepared, for the carbon nanotube growth a flow of 10 % C_2H_2 was introduced into the chamber instead of H_2 and the temperature was increased. In our experiments two different temperatures were experimented in the CVD process for the carbon nanotube growth: 600 °C and 750 °C. Carbon nanotube growth time was chosen to be between 30 minutes to 2 hours.

Basically the reaction occurring in the reactor is:

$$C_2H_2 \longrightarrow 2C + H_2$$

In the decomposition of acetylene, carbon molecules are deposited on the iron catalysts placed on silica plates. The reactions are carried out at temperatures mentioned above. These temperatures are selected referring to the literature.

A total CVD (figure 3.1) experiment, including the catalyst pretreatment, takes between 16 to 18 hours. Through out the whole experiment the vacuum pump works constantly and the pressure of the system is held constant by a valve. The thermocouple used in the system is Pt-Rh type thermocouple that is capable of measuring up to 1200 °C, and is connected to a PID temperature controller powering the oven.

Flowrates of the gases are controlled by rotameters connected to the system by ¼ inch copper pipes. A total flowrate of 110 ml/min is maintained at the system; 100 ml/min N_2 and 10 ml/min C_2H_2. Also in the pretreatment of catalyst stage the flowrates of N_2 is again 100 ml/min and H_2 10 ml/min.

3.3 Electron Beam (e-beam) Method

In this method, after the catalyst coated plates were prepared as described above, the plates were placed in the three different locations in the

system. Only catalyst coated plates were used in this system instead of powder type catalyst since the system is not suitable for this type of catalyst. The system is consisted of three cylindrical electrodes and a quartz tube. In the operation, while a glow DC discharge is operating between the cathode and the anode in the middle, between the cathode and the other anode by applying a pulsed high voltage the electrons were accelerated and an e-beam was obtained in the glow discharge zone. Acetylene gas was used as the carbon source as was in the CVD method. In this system the low pressure acetylene gas was introduced in the system and the carbon and hydrogen dissociation was achieved by applying a pulsed high voltage to the gas. Consequently, the carbon atoms in the plasma were deposited on to the catalyst coated plates that were placed in the cathode and at two anode zones.

The e-beam setup is constructed by Hilal Göktaş at METU physics department. The system is described in detail in the article by Göktaş et al. in 2002 (figure 3.2) [61].

3.4 Characterization techniques

One of the difficulties in the carbon nanotube production is the characterization because of their nanometer scale dimensions. In our experiments Transmission Electron Microscopy (TEM) and Raman Spectroscopy techniques were used for the characterization of the samples.

3.4.1 Transmission Electron Microscopy (TEM)

For the Transmission electron microscopy (TEM) JEOL 100C 100 kV TEM in the TUBITAK-MAM laboratories were used. For the TEM characterization the samples were prepared in order to have TEM images. Since the substrates could not be introduced into the microscope the carbon deposit on the silica plates were taken into an ethanol suspension by sonification. Sonification was done by Bandelin Sonorex RK100H 35 kHz frequency ultrasound water bath.

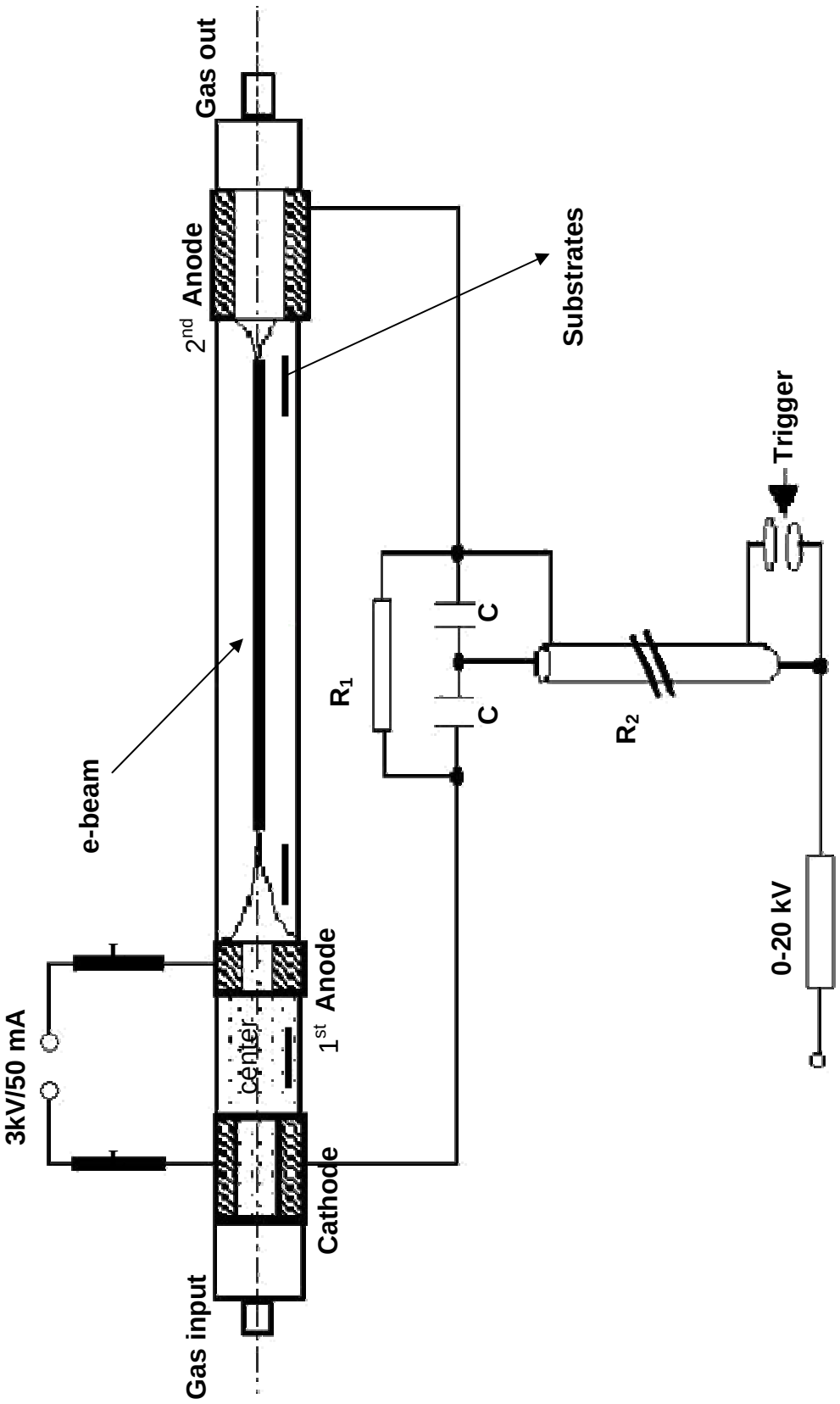

Figure 3.2 Schematic representation of the electron beam system.

Then the suspension was drop dried on to the carbon film coated TEM grids.

3.4.2 Raman Spectroscopy

Raman spectroscopy is one of the most important characterization technique since the nanotubes, both single-walled and multi-walled, gives characteristic peaks. In the characterization of the samples the Raman spectroscopy at KOC University (BRUKER RFS100/S Nd: YAG-Laser with 10-20 mW laser energy) and at BILKENT University (Ar^+ laser with 5 mW laser energy) were used. The samples to be inspected in the Raman spectroscopy does not need any further treatment as they can be characterized as taken from the production systems.

CHAPTER 4

RESULTS AND DISCUSSION

When carbon nanotubes are in concern characterization becomes to be the most important and most difficult part of the research. In this research, for the characterization of the CNTs transmission electron microscopy (TEM) and Raman spectroscopy was used.

4.1 Transmission Electron Microscopy (TEM)

Here are some examples of TEM images for the experiments done by CVD and e-beam systems. In order to characterize the deposits on the silica plates by TEM, the deposited material should be taken on to the TEM grids. The deposits were taken from the silica plates by sonication of the plates in suspension, as mentioned in Chapter 3. In sections 4.1.1 and 4.1.2 TEM images of CVD samples and e-beam samples are given respectively.

According to the TEM images presented in the below sections, only MWNTs were synthesized in both of the processes. However, the Raman spectra results in section 4.2 show the existence of SWNTs. This was because of the TEM device used. In the TEM characterization experiments although the smaller nanotubes were observed at higher magnifications more than 100,000, the images could not have been taken because of the limitations of the device.

4.1.1 CVD

The TEM images from figure 4.1 to 4.11 all belong to samples from CVD experiments carried out at 600 °C using iron catalyst deposited on the

silica plates by sol-gel method, except figure 4.2. Figure 4.2 belongs to a MWNT that was produced by iron catalyst deposited quartz wool. It is almost impossible to get TEM pictures with good resolution from silica plates though they were thinned down to 200 µm. So, we have tried to use quartz wool to deposit nanotubes. Although the electrons could pass through the quartz wool, they scattered from the quartz walls preventing to capture images. So we quitted to take direct pictures from silica substrates, either plate or wool. The nanotubes were taken into suspension by ethyl alcohol in an ultrasound sonification device. After sonification it was noticed that the suspension from quartz wool sample was more than that of silica plates. However, most of the deposit on the quartz wool was carbon impurities rather than CNTs.

A very long MWNT can be seen in the figure 4.1 that was produced by CVD process at 600°C. The length of this CNT is about ~5µm which is much longer when compared to other observed CNTs presented in the other figures. In figure 4.2, a shorter CNT can be seen with some impurities around its surface. This nanotube is a sample of CNTs grown on the iron coated quartz wool. This is a MWNT with outer diameter (OD) of ~50 nm and an inner diameter (ID) of about ~5 nm.

In figure 4.3, two MWNTs can be seen. The catalyst particle probably split into two, growing two tubes in the opposite directions from the same origin. These nanotubes have ODs of ~40 nm and IDs of about 4-5 nm. In the following figure (figure 4.4) another MWNT is shown which was bent in the middle. The curvature in this nanotube was caused either by the system conditions or probably by the sonification of the substrates.

Amorphous carbon structures were also observed together with the CNTs in TEM images. In figure 4.5 two spherical carbon structures are seen together with a MWNT. These spherical particles are thought to be carbon particles. These structures may also be some kind of a giant fullerene cluster.

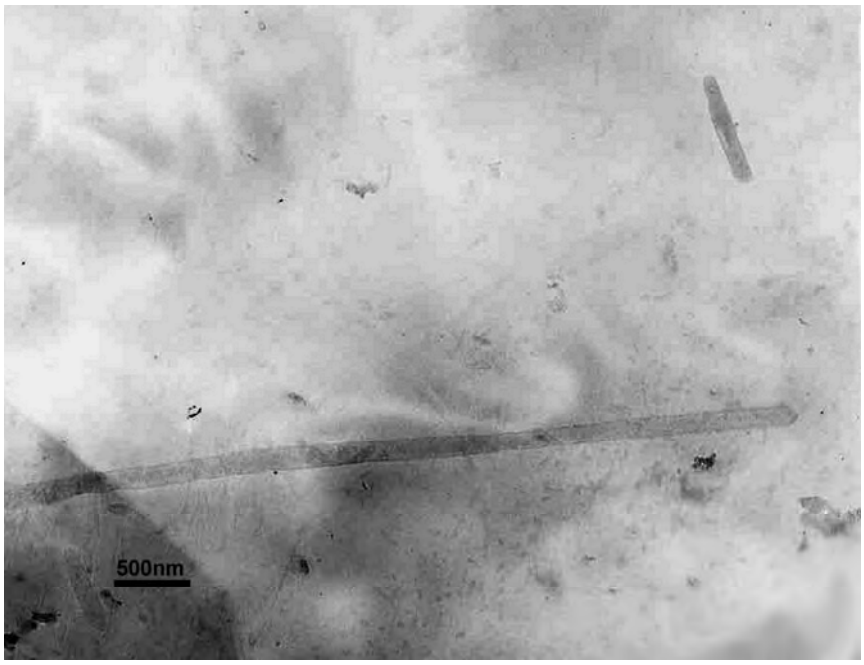

Figure 4.1 A MWNT with an outer diameter of ~100 nm and ~5 µm long. Magnification x10k.

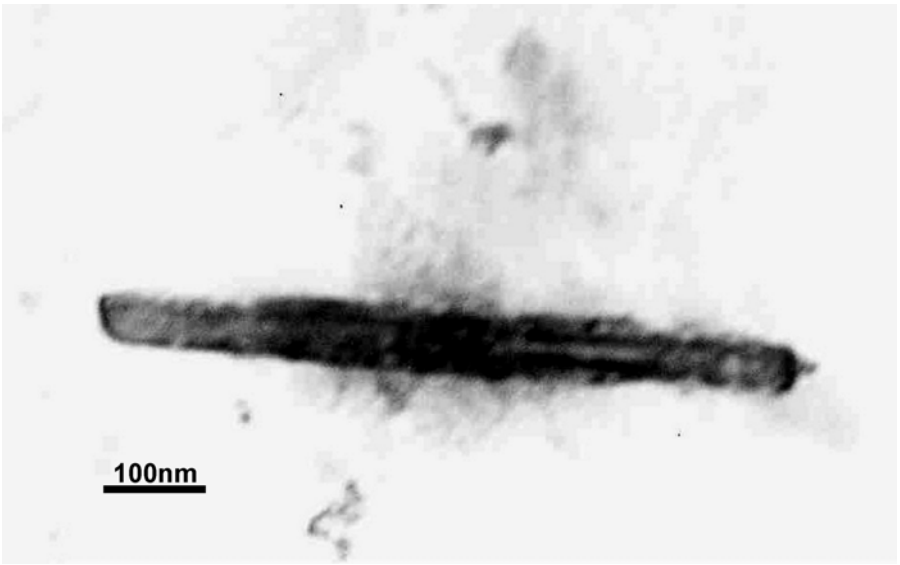

Figure 4.2 A MWNT with OD ~50 nm and ID ~5 nm and a length of ~1 µm. There are some impurities in the middle. Magnification x66k.

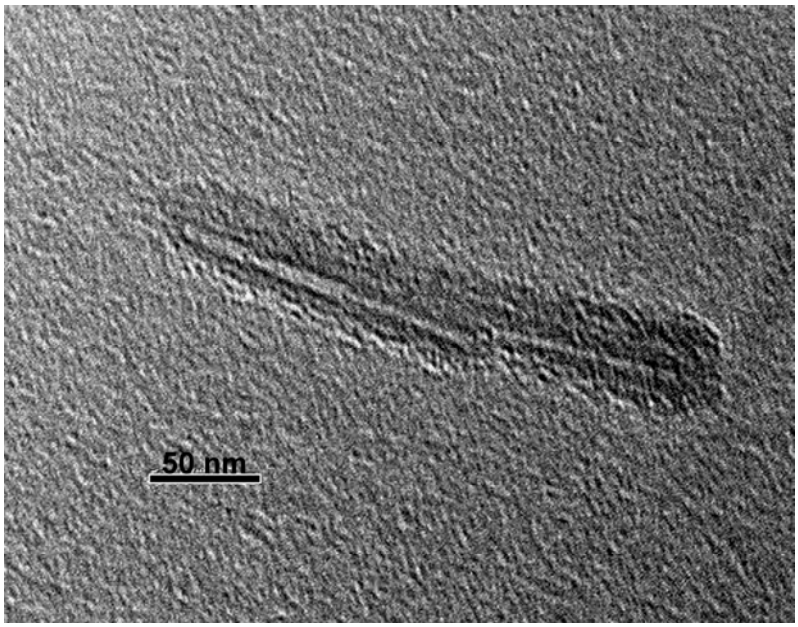

Figure 4.3 Two MWNTs grown on the same catalyst particle in the middle towards opposite directions. OD= ~40 nm and ID= ~4-5 nm.

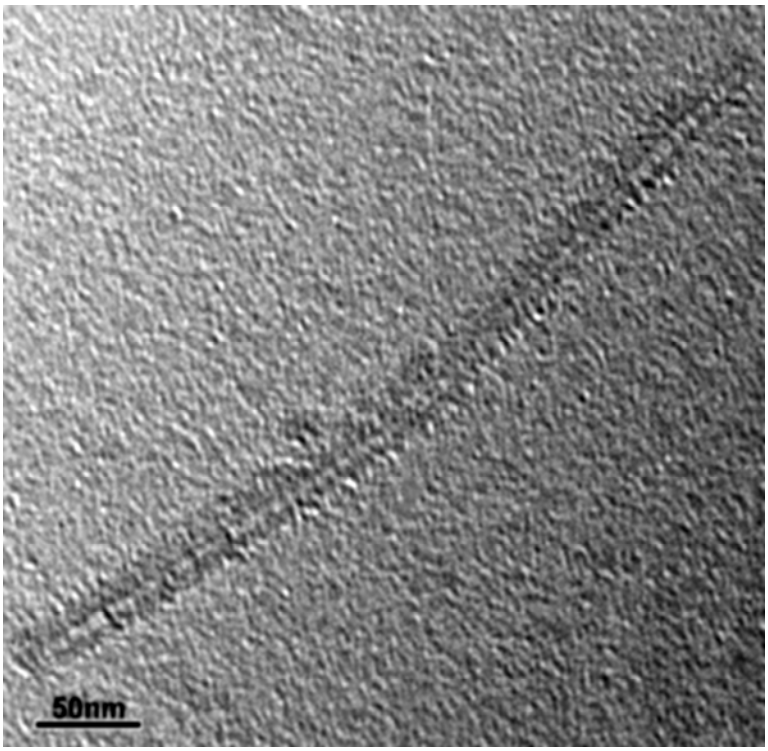

Figure 4.4 Another MWNT that is a little bent in the middle. This nanotube has an OD of ~30 nm and an ID of ~5 nm.

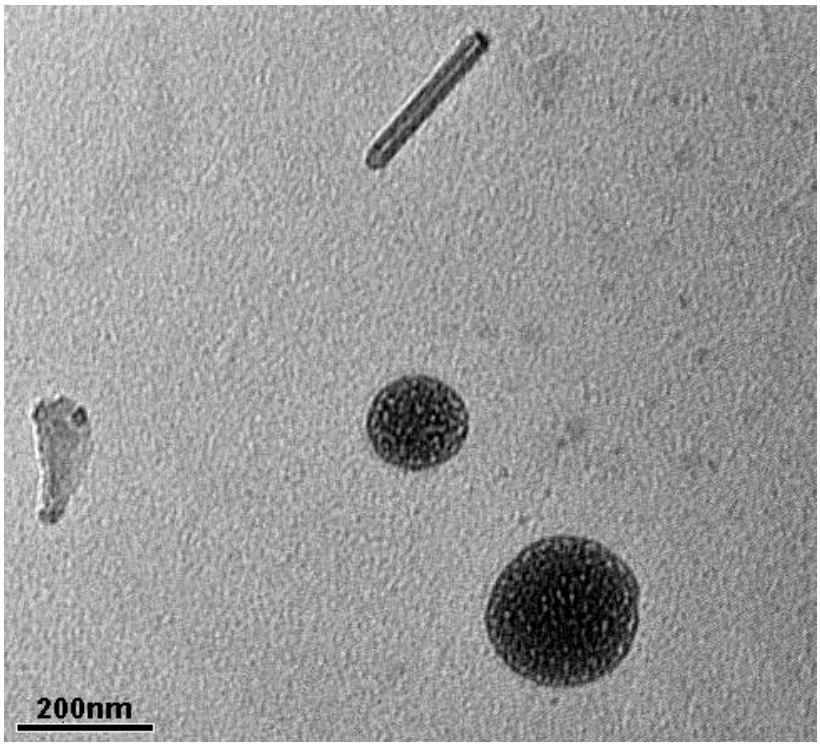

Figure 4.5 A short MWNT and two spherical particles possibly carbon black particles.

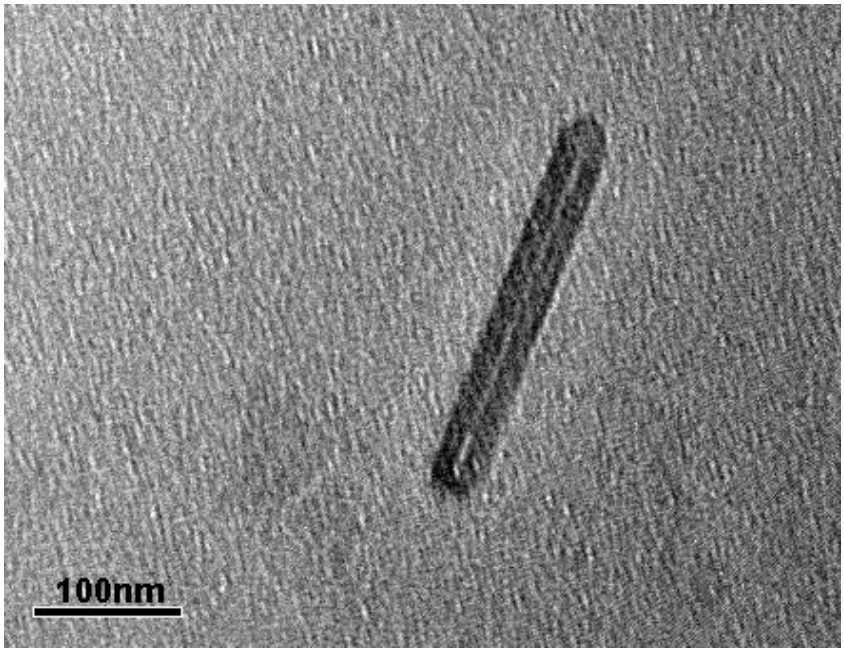

Figure 4.6 A closer image of the MWNT that was shown in the previous image (figure 4.5) having an OD of ~35 nm and an ID of ~4 nm.

A closer image of the MWNT seen in figure 4.5 is given in figure 4.6 which is half a micron in length and has an OD of ~35 nm and an ID of ~4 nm. In this image the innermost tube can clearly be seen.

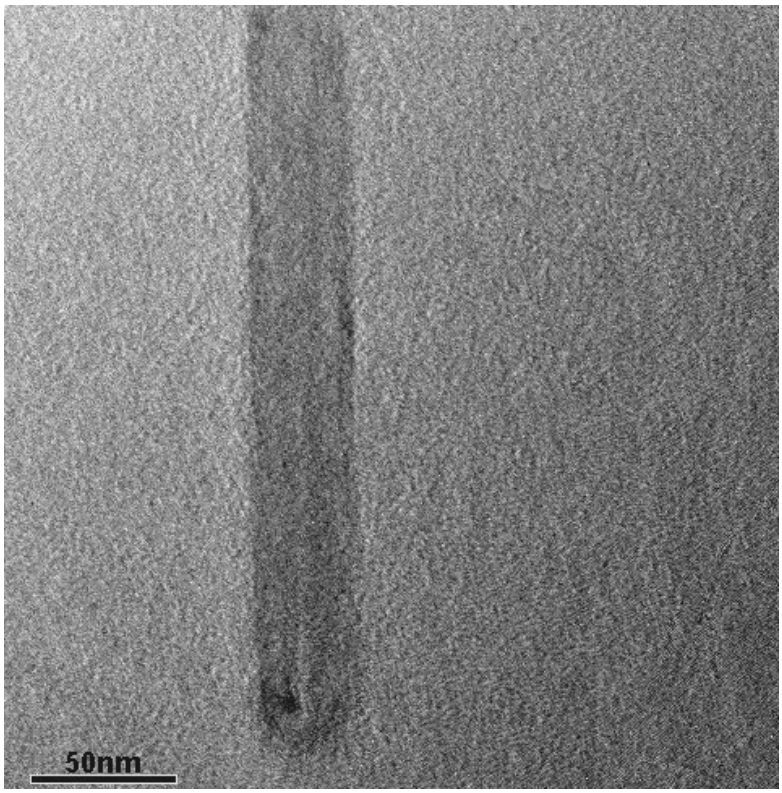

Figure 4.7 In this image the catalyst particle on which the nanotube has been grown can be seen (the black dot at the bottom). OD= ~40 nm and ID= ~4 nm.

The images in figures 4.7 and 4.8 belong to the same MWNT with ~40 nm OD and ~4 nm ID. In these images the black dot, shown by an arrow in figure 4.8, at the tip of the nanotube is the iron particle that catalyzes the nanotube growth and moves at the tip of the tube. In both of the images, especially in figure 4.8, the curvature of the innermost tube of the nanotube around the catalyst is clearly seen. This curvature shows that this nanotube was grown according to the tip growth described in figure 2.15.

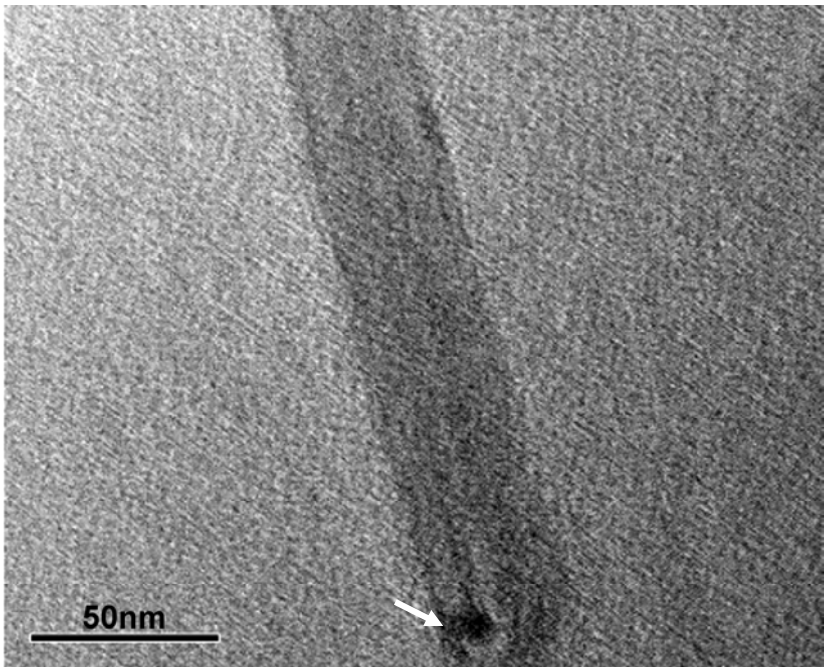

Figure 4.8 Image of a MWNT again the catalyst particle can easily be seen.

Figure 4.9 shows two images of a MWNT with an OD of ~40 nm and an ID of ~4 nm. In this nanotube one of the tips is conical whereas the other is not. This type of tips is named ‘nanohorns’, and research is carried on to use them as electrodes of fuel cells. However, nanohorn structures are not usually seen in the multi-walled nanotubes. The iron catalyst particle can also be seen in the conical tip of the MWNT.

In figure 4.10 an interesting carbon nanotube is seen. This nanotube, or better called a ‘tubular carbon nanostructure’, has curled up branches at one side of it. The innermost tube of the nanotube with a diameter of ~4 nm can be seen clearly in the image.

The structures seen in figure 4.11 is onion like spherical structures with different diameters grown on catalyst particles. These structures are also thought to be possible torus structures.

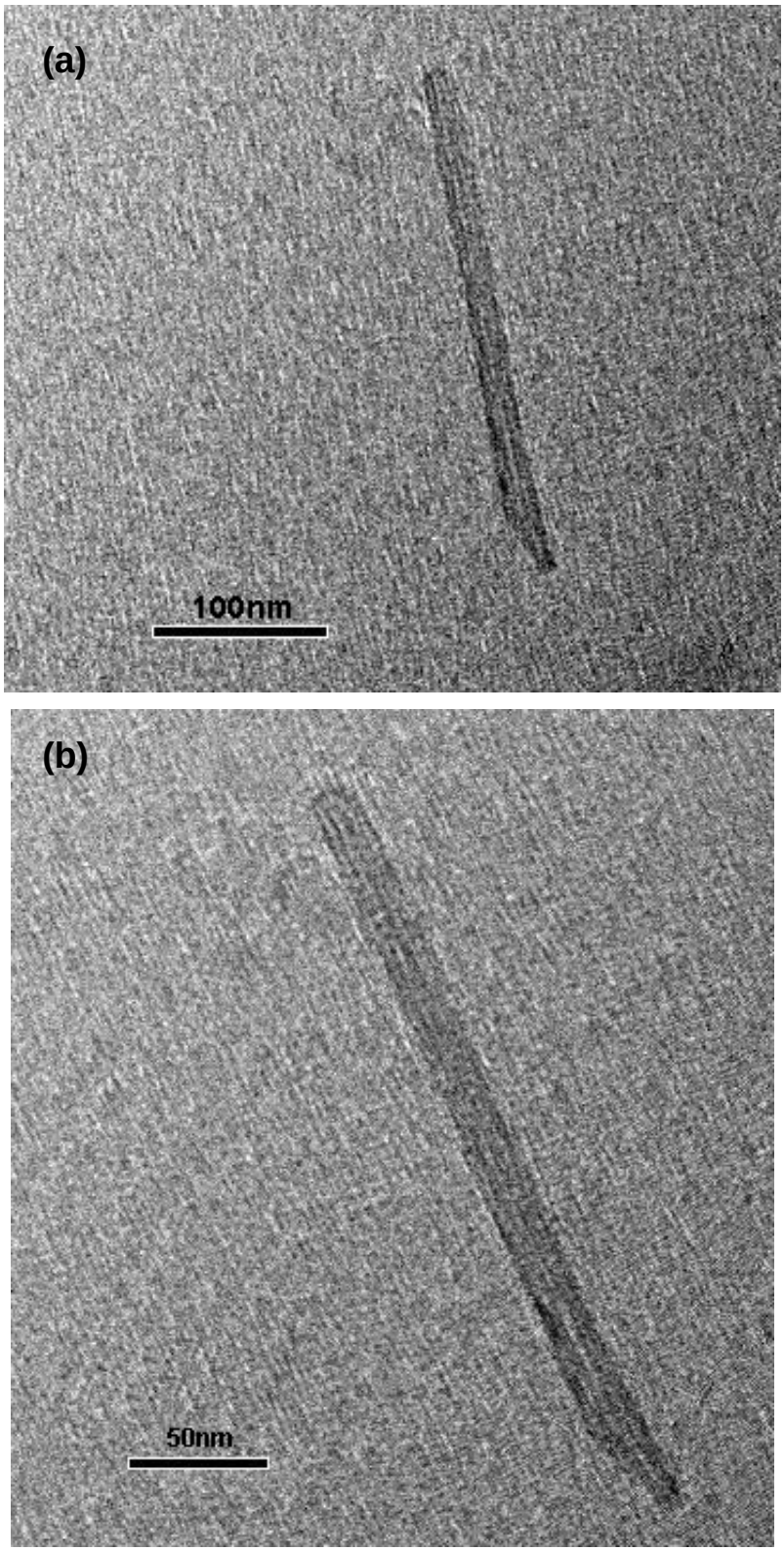

Figure 4.9 The above images **(a)** and **(b)** belong to the same MWNT with an OD of ~ 40 nm and an ID of ~4 nm.

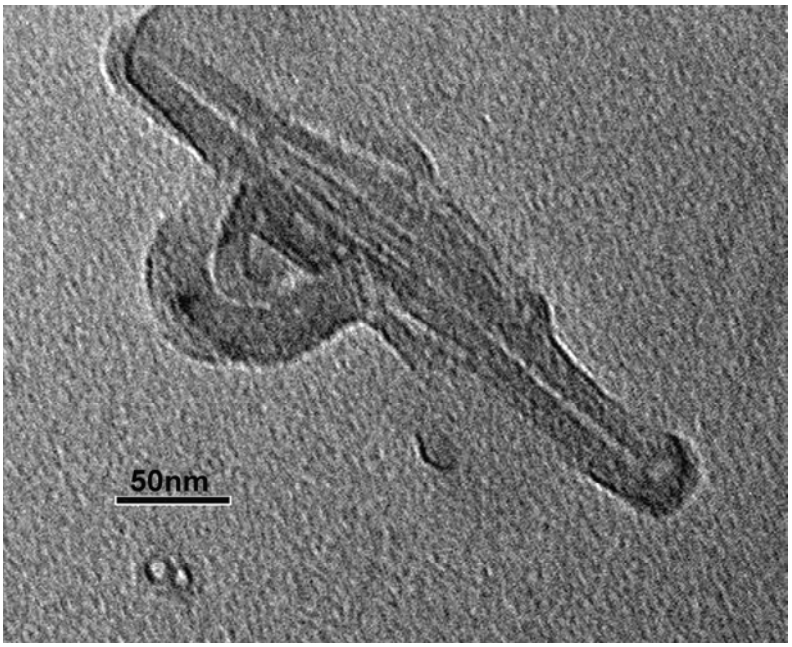

Figure 4.10 An interesting MWNT that is deformed and branched.

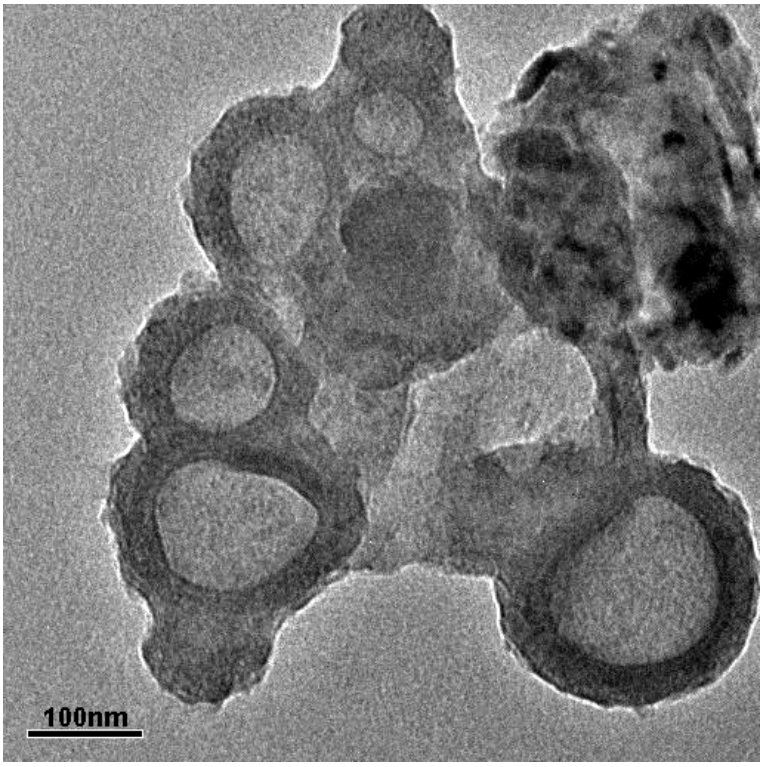

Figure 4.11 An interesting structure observed in the CVD deposits. The rings are possibly onion structures of carbon and the structure at the above right corner is the catalytic surface.

In summary, we observed that there are images of different multi-walled carbon nanotubes with different inner (3-5 nm) and outer (30-100nm) diameters, and different lengths changing from several hundreds of nanometers to several microns. In some of the images, catalyst particles, on which the carbon nanotube was grown, were also observed; showing that this is a catalytic process. Generally CNTs, grown by CVD process are expected to be straight as can be seen in the figures above. However, there are also some other nanotubes produced in the system as shown in figures 4.4 and 4.10 and also some other amorphous carbon structures are produced (figure 4.5 and 4.11).

4.1.2 Electron Beam (e-beam)

In the below sections (4.1.2.1 – 4.1.2.3) the TEM images of samples from the e-beam system were given according to the location of the substrate in the system. These three places are: (i) before 2nd anode, (ii) after first anode, and (iii) center positions (see figure 3.2).

In this process, the deposit on the silica plates after the experiment was much less compared to that of in CVD process. This might be due to the reason e-beam system produces deposits clear off impurities.

4.1.2.1 Substrate Positioned Before the 2nd Anode

The deposition occurs with a very high rate when the silica substrate was positioned before the 2nd anode.

This location is the coolest zone of the system. Actually the temperature of the whole system increase slightly as compared to the room temperature. However, no significant difference in the temperature of this part of the system was noticed.

In figures 4.12, 4.13, and 4.14 the images many carbon nanotubes piled up on each other are seen at different magnifications. Some of the structures in these images are thought to be cylindrical carbon fibers as they are considerably thick.

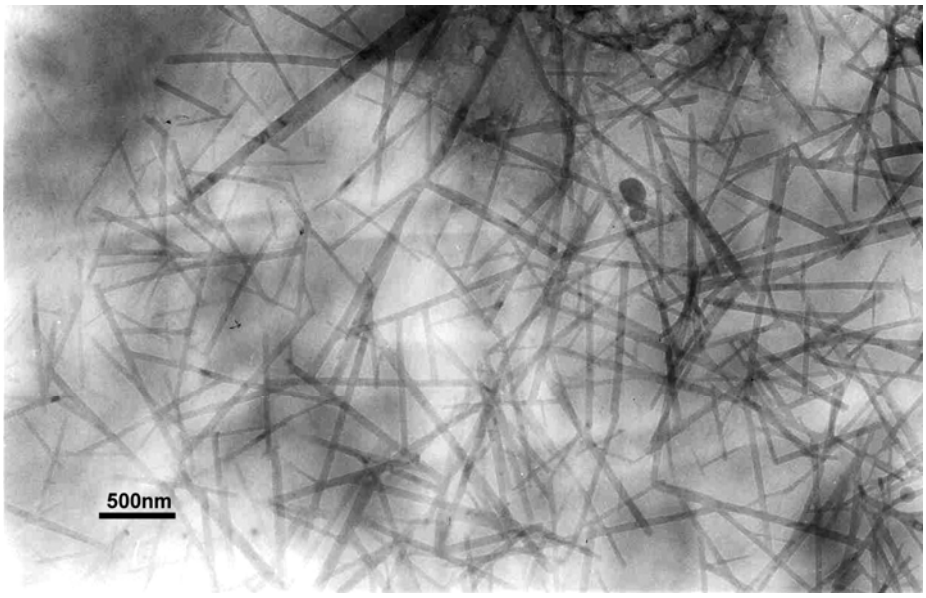

Figure 4.12 A pile of nanotubes, in various sizes, produced by e-beam system. Magnification x13k.

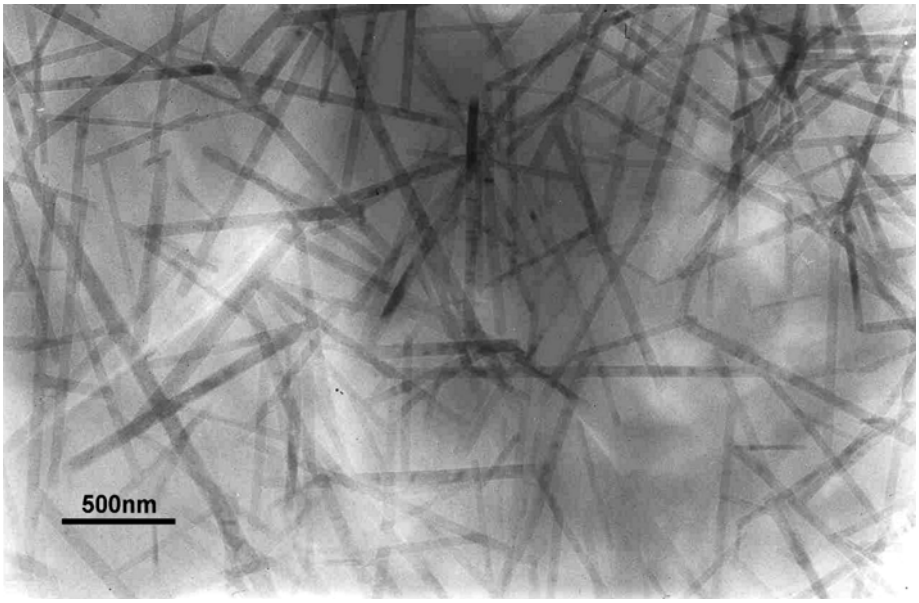

Figure 4.13 Another image of a pile of nanotubes taken from another sample. Magnification x20k.

In figure 4.15, an image of a bamboo structured carbon nanotube with a ~40 nm of diameter and approximately 2 μm of length is shown.

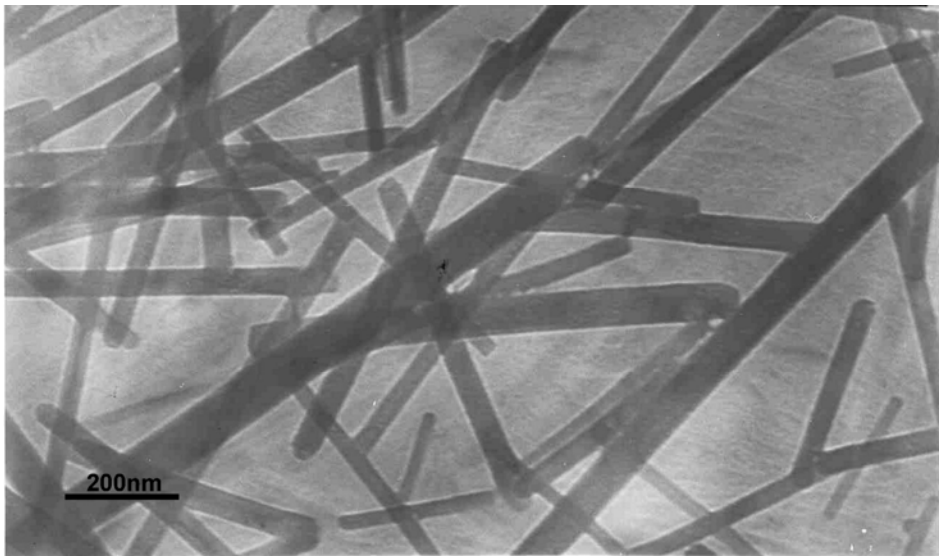

Figure 4.14 A closer view from figure 4.12. Magnification x50k.

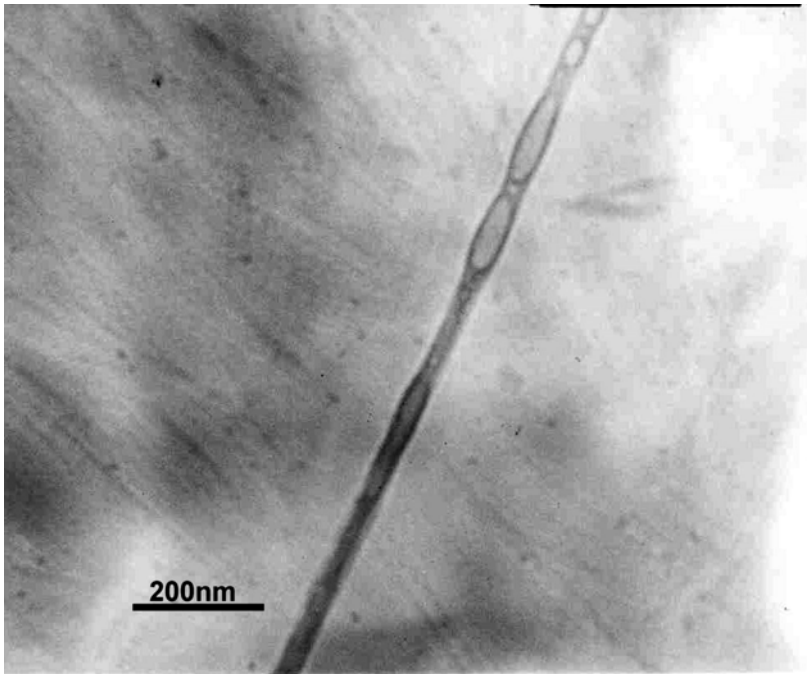

Figure 4.15 A CNT having various diameter distributions along with some bamboo like structure. OD= ~40nm and Length= ~2µm. Magnification x50k.

In figure 4.16, again a bamboo structured CNT with a conical, nanohorn like, tip is seen. The magnified view (i.e. smaller picture) shows that there exists another tube inside it with a diameter of ~40 nm.

Figure 4.17 shows a pile of cylindrical fibers (nanorods). They have giant diameters; therefore they are probable cylindrical carbon fibers.

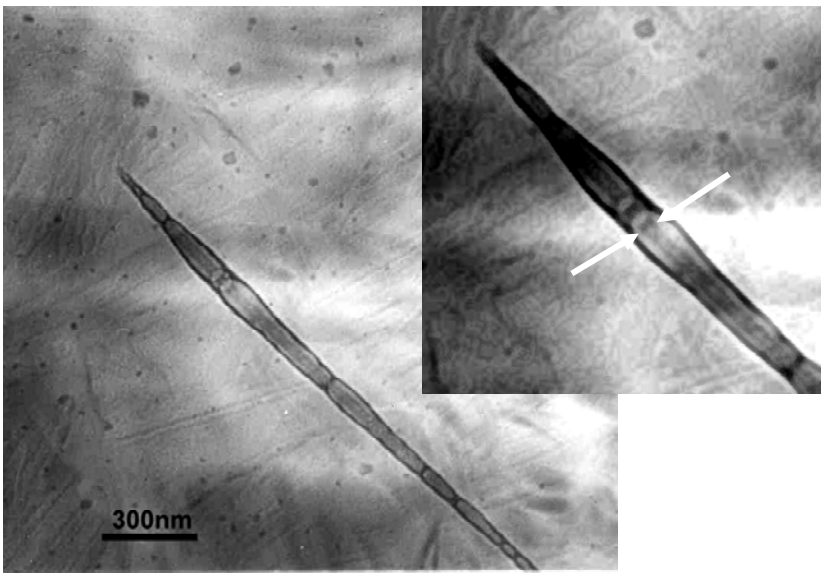

Figure 4.16 A nanohorn structure with a nanotube inside the nanohorn having an OD of ~40nm. Magnification x26k.

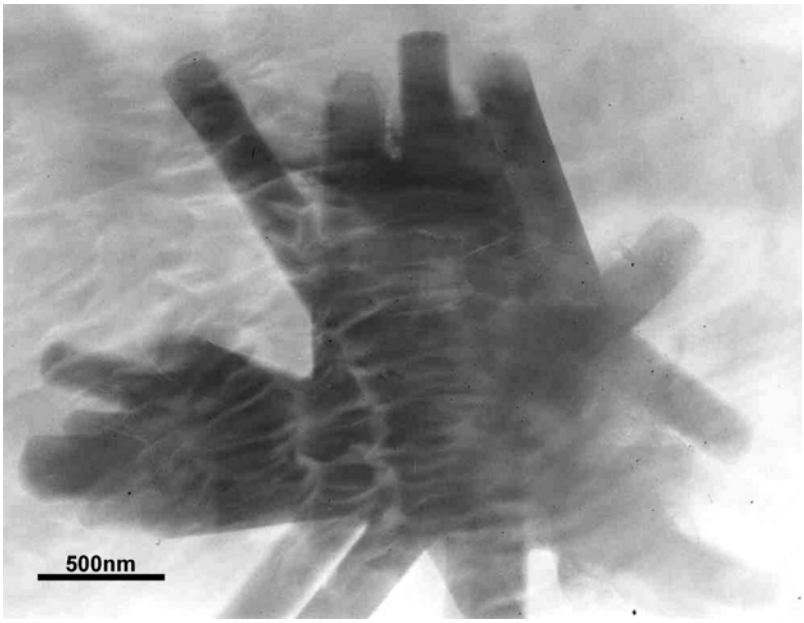

Figure 4.17 A block of nanorods produced by the e-beam system stick to each other probably because of the suspension used in the sonication. Magnification x20k.

Short length fibers were observed also on the substrate. Figure 4.18 shows these fibers.

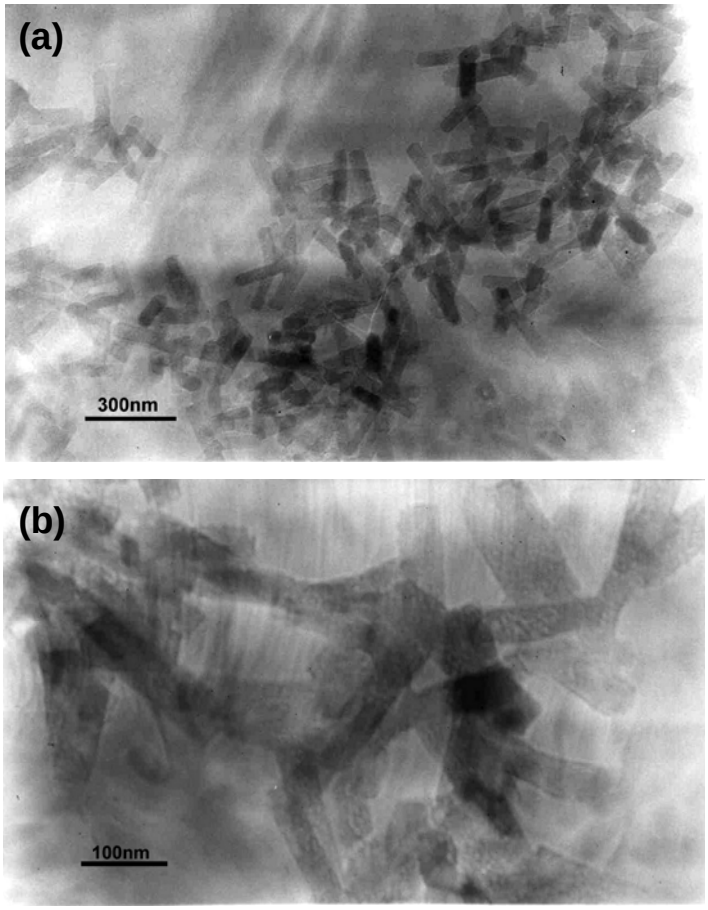

Figure 4.18 Some other structures of carbon. (b) It can be seen that they are porous structures. (a) Magnification x33k. (b) Magnification x100k.

In this part of the system a variety of structures were observed in the TEM images. Apart from CNTs, nanohorn (figure 4.16) and some amorphous porous structures (figure 4.18) were observed.

4.1.2.2 Substrate Positioned After the 1st Anode

Little carbon deposition took place in this zone. Carbon nanotubes formed also in this zone as seen from figure 4.19 and 4.20. The observed

nanotubes have diameters of 100 nm, and were generally vertically stacked as seen from figure 4.20.

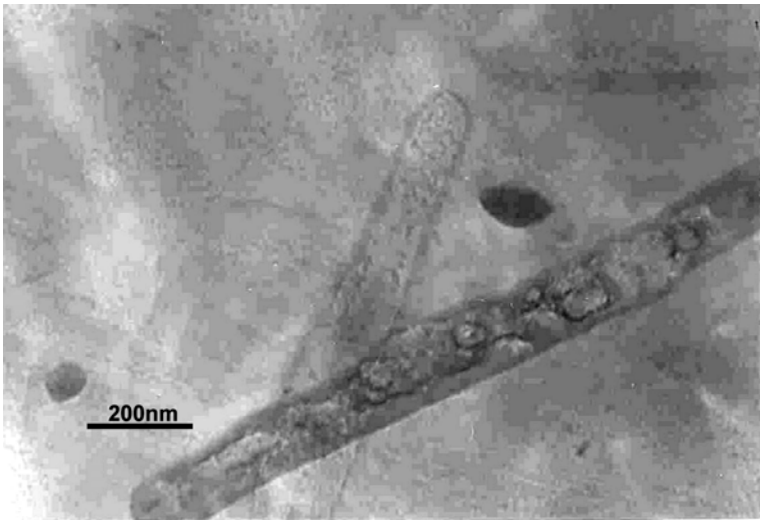

Figure 4.19 Two large CNTs, one on another, with diameters close to ~100 nm. Magnification x50k.

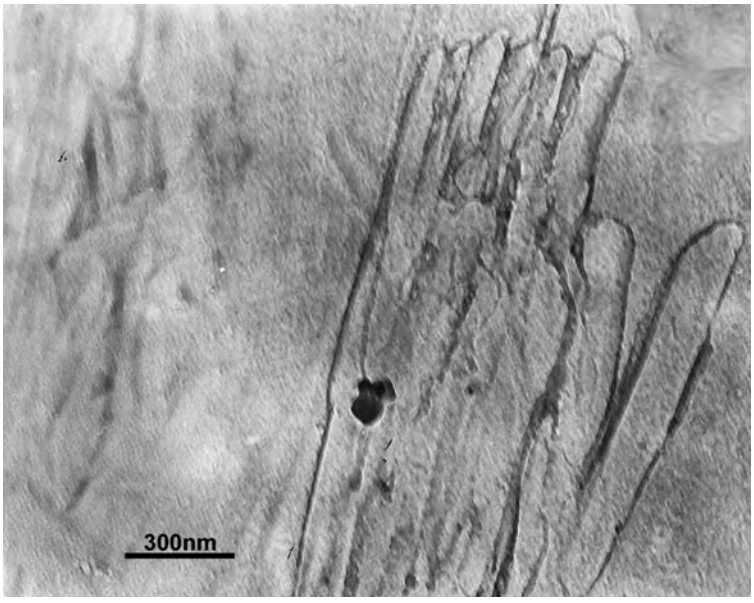

Figure 4.20 A pile of CNTs, stick together side by side, having diameters ~100 nm. Magnification x33k.

4.1.2.3 Substrates Positioned at the Center

The gas enters to the system from the cathode and it decomposes into fragments and carbon atoms. The temperature of this part increased during the experiment. The carbon deposition on the substrates placed at this zone was more than that of other zones.

The images showed a variety of deposits both cylindrical carbon fibers and carbon nanotubes.

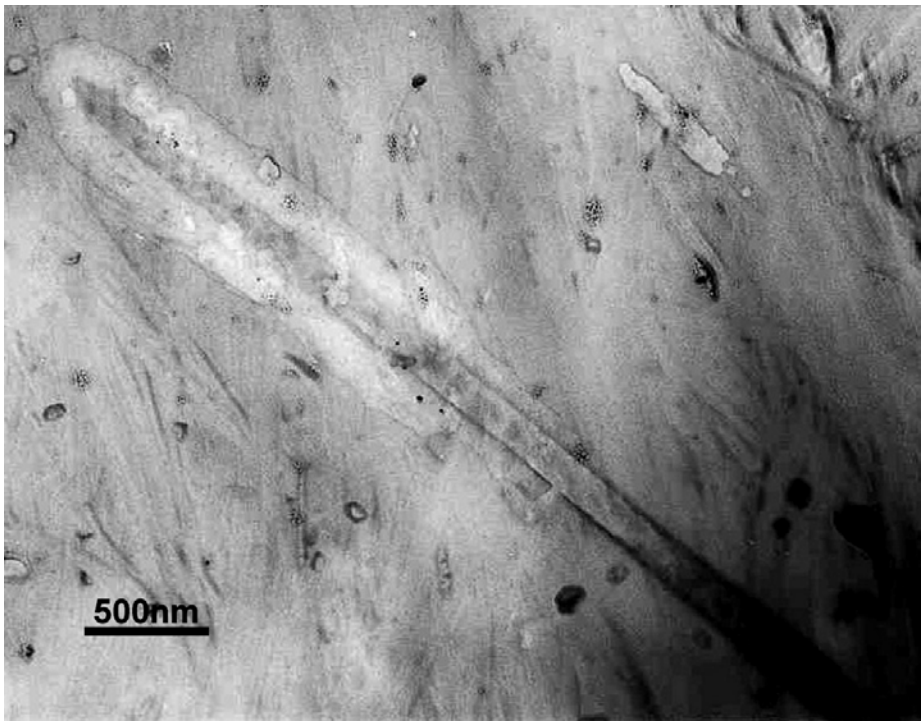

Figure 4.21 A large carbon nanotube produced by e-beam system at the cathode part. Magnification x13k.

A big CNT produced is seen in figure 4.21. Smaller CNTs are barely observed in the background in figure 4.22. There are three large diameter and one small diameter objects in figure 4.23. The small diameter object is probably CNT. The large diameter ones seem to be CNT, as they look like empty inside. However, to our knowledge there is no such large diameter CNT reported in the literature. It might be possible to synthesize such large diameter CNTs by e-beam method. Further investigations need to be done

on these objects. Figure 4.24 is a higher magnification image of nanofibers in the figure 4.23.

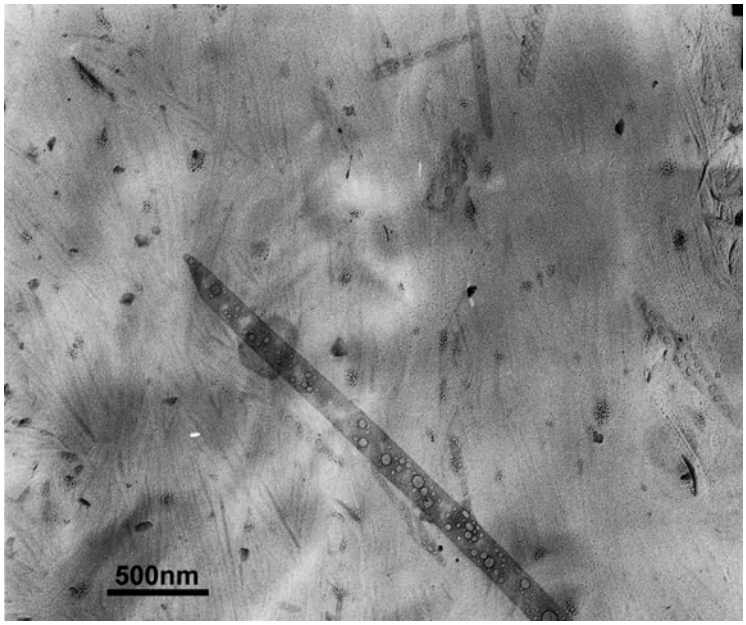

Figure 4.22 Another large CNT and small CNTs at the above part of image. Magnification x16k.

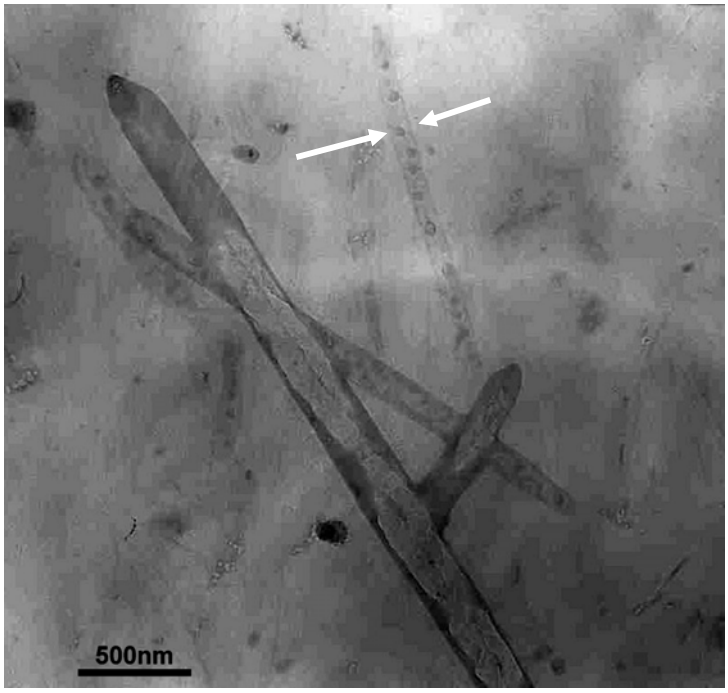

Figure 4.23 Three large nanofibers and behind them a smaller CNT can be seen. Magnification x16k.

A nanohorn structure is seen in figure 4.25 with the catalyst particle shown by the arrow. This nanotube has probably been grown with the root growth.

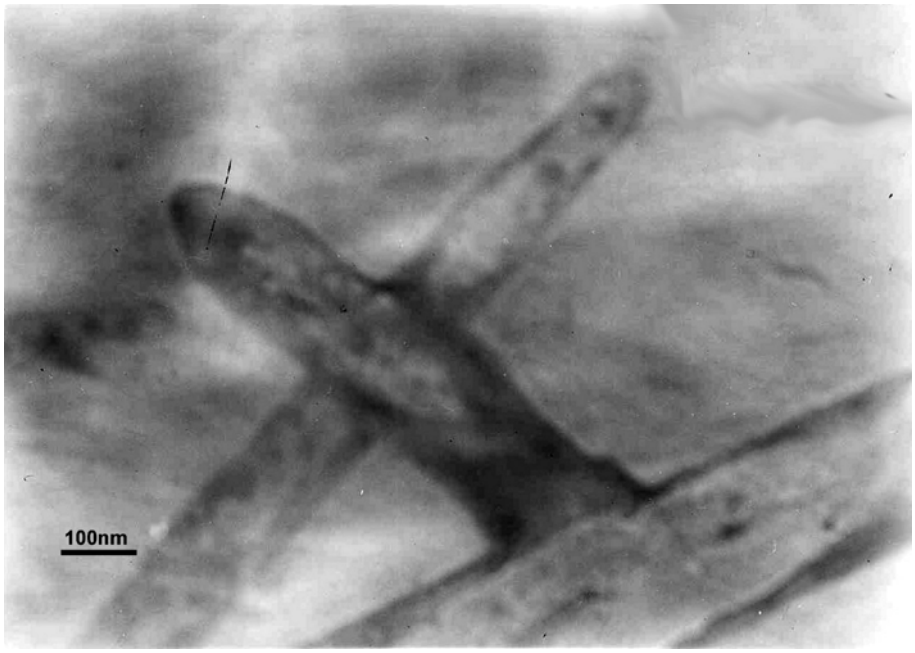

Figure 4.24 A higher magnification image of the three nanotubes in figure 4.23. Magnification x66k.

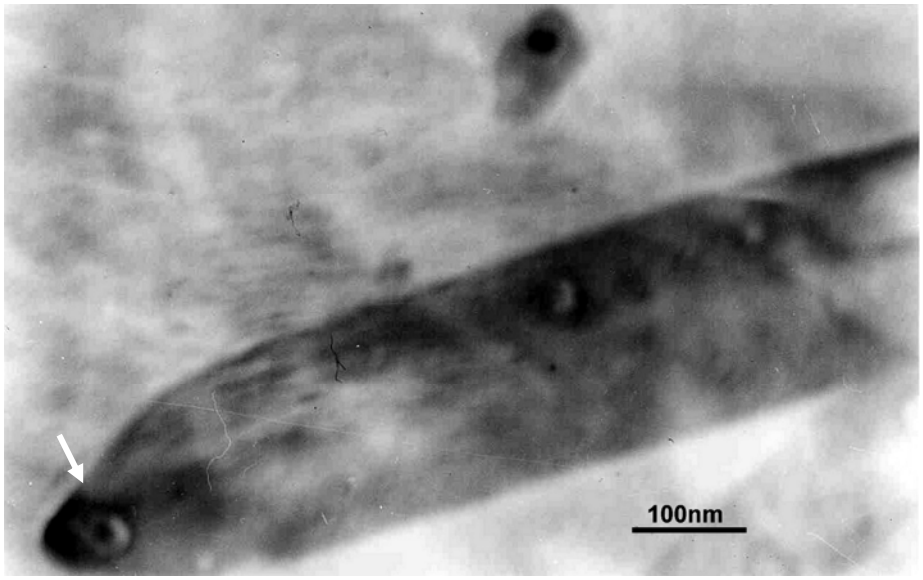

Figure 4.25 A nanohorn structure with 200 nm OD. The catalyst particle can be seen at the tip of the structure. Magnification x100k.

In figures 4.26 and 4.27 bubbles were observed inside the tube. These bubbles should be due to ethanol suspending the tubes. It seems that nanotubes are permeable to small size organic molecules. There could be some atomic size deficiencies on the structure which let ethanol inside.

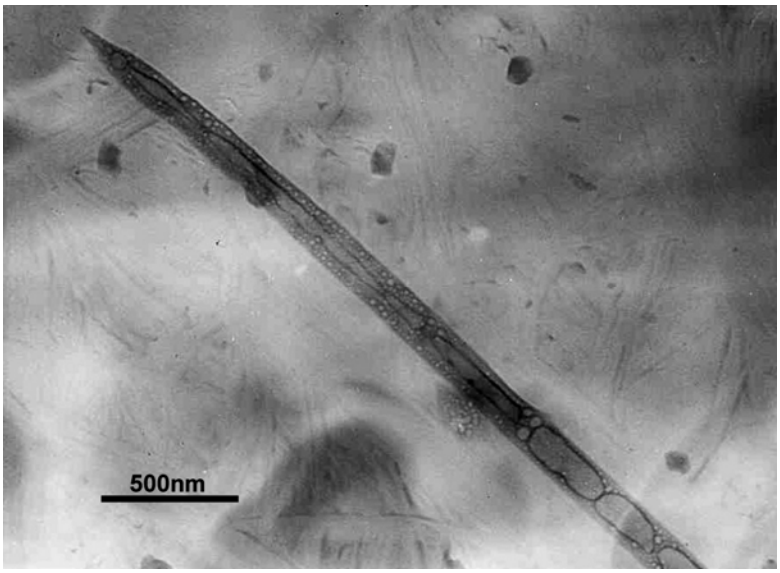

Figure 4.26 Another nanohorn structure which has absorbed the suspension. Magnification x20k.

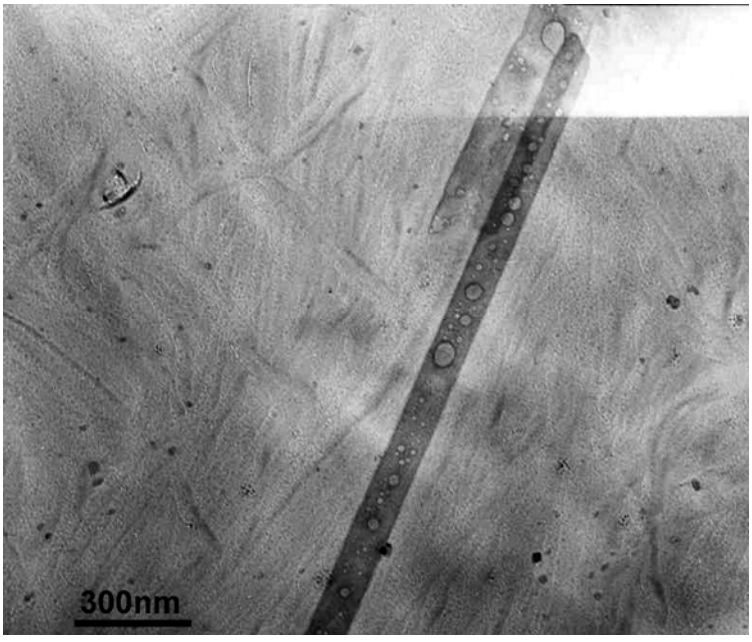

Figure 4.27 A CNT that has absorbed the suspension. Magnification x26k.

The entrance of ethanol through hexagonal (i.e. honeycomb) carbon structure can also be considered, but theoretical and experimental investigations are needed to make further comments.

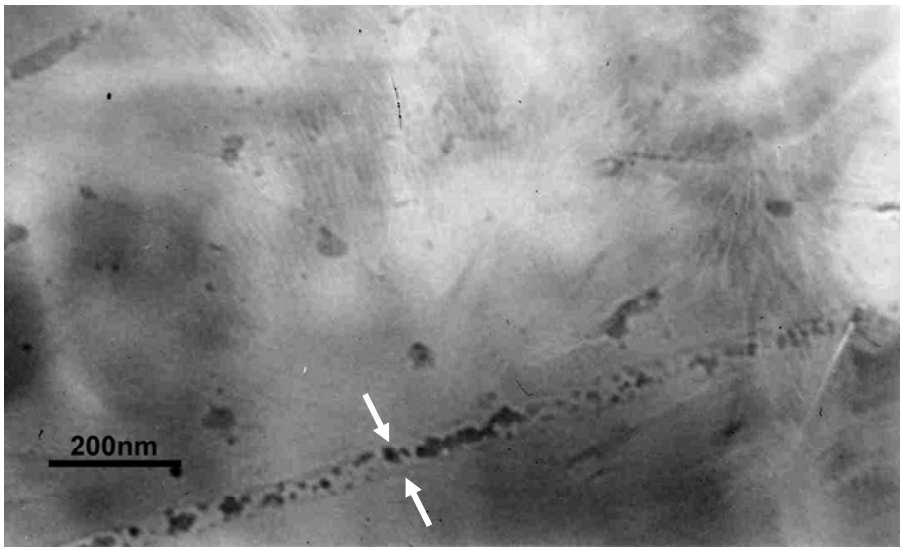

Figure 4.28 A CNT with ~50nm OD and length more than ~1µm. Magnification x50k.

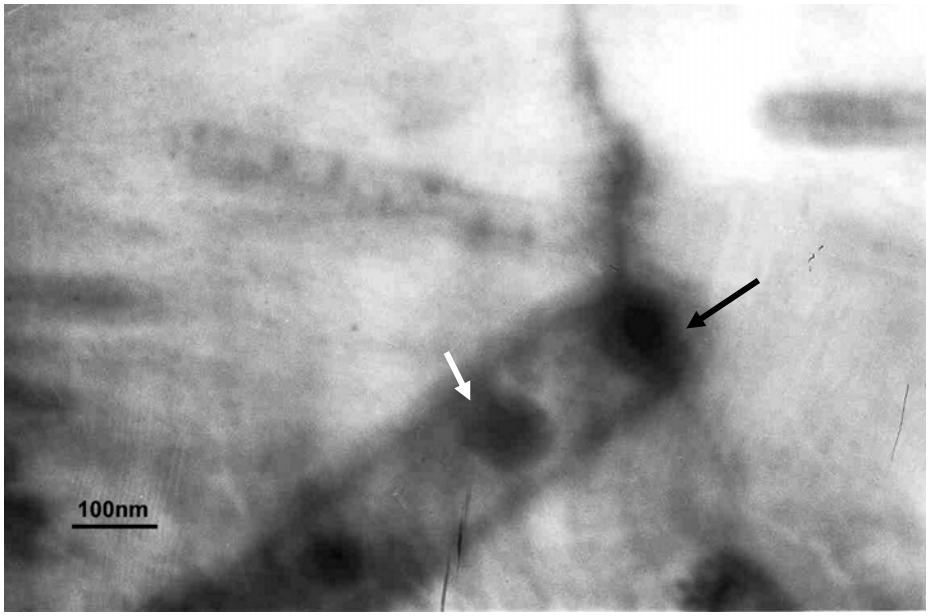

Figure 4.29 An image of tip of a CNT with ~150nm. The black dot shown by the black arrow is the catalyst particle. White arrow shows an amorphous carbon particle inside the CNT. Magnification x66k.

Figure 4.28 is an image of CNT having a diameter of ~50 nm and a length of more than 1 µm. The arrows show the walls of the nanotubes. It is highly filled inside.

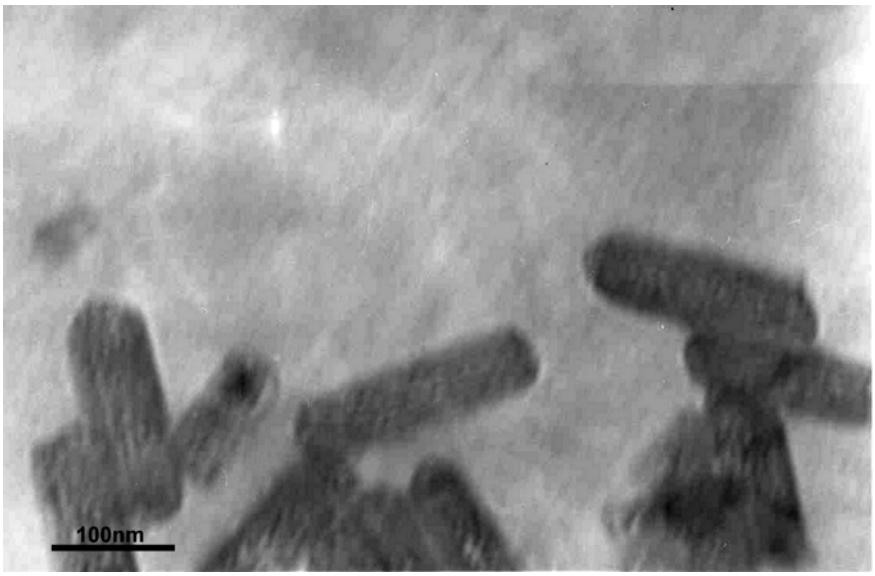

Figure 4.30 Same particles as observed in the samples placed at the anode at the end. Magnification x100k.

In figure 4.29 the catalyst particle (black arrow) at the tip of the CNT is seen clearly. However, a spherical particle (white arrow) placed inside the nanotube is also seen.

The images show that some other structures have also been produced in this part of the system as was mentioned earlier. Some porous carbon structures were also observed (figure 4.30) which had also been observed in figure 4.18.

4.2 Raman Spectroscopy

Another important characterization method for the characterization of CNTs is the Raman spectroscopy. In this research, two different Raman spectroscopy devices were used with different lasers: Ar^+ ion laser and Nd: YAG laser.

Figure 4.31 is the Raman spectrum of CVD specimens. All the peaks except the one at 303 nm are the characteristic peaks of single-walled carbon nanotubes. The one at 303 nm is of SiO_2 [33].

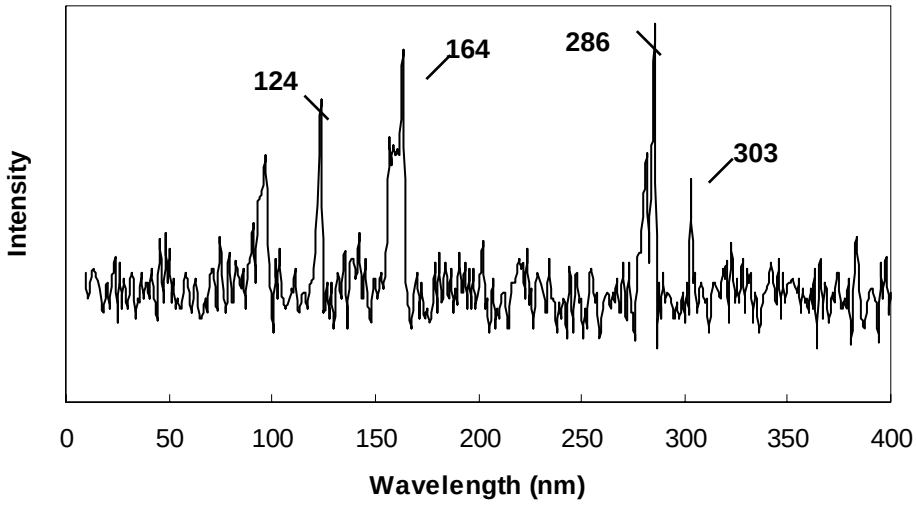

Figure 4.31 RBM peaks for samples from the 600°C CVD experiments.

Figure 4.32 is the Raman spectrum of e-beam specimen positioned before 2nd anode. The peak at 180 nm refers to SWNT [31].

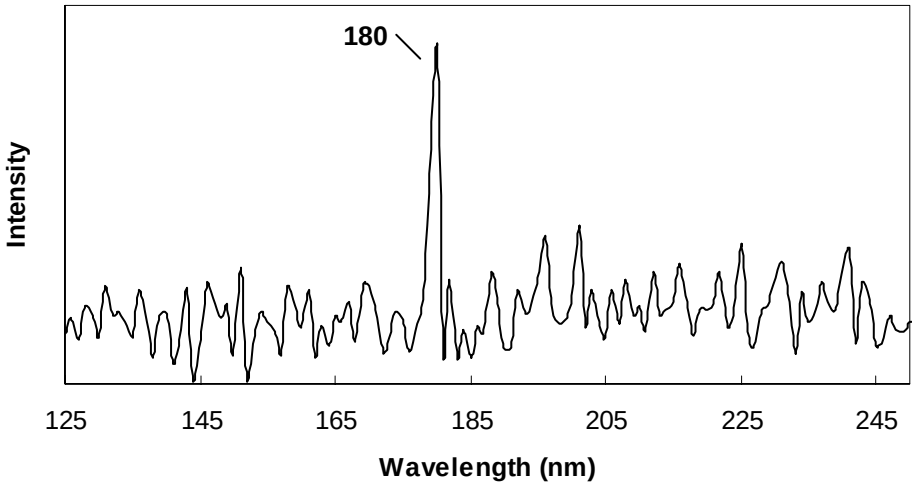

Figure 4.32 RBM modes of the specimen positioned before the 2nd anode of the e-beam setup.

In figure 4.33 the Raman spectrum of MWNTs produced by e-beam can be seen. The general G-band MWNT peak was observed at wavelengths between 1570-1620 nm [30]. The peak seen in figure 4.33 has a wavelength of 1648 nm. It is thought that the laser wavelength caused interference and shifted the peak to the left. Such deviations were observed in the literature [36].

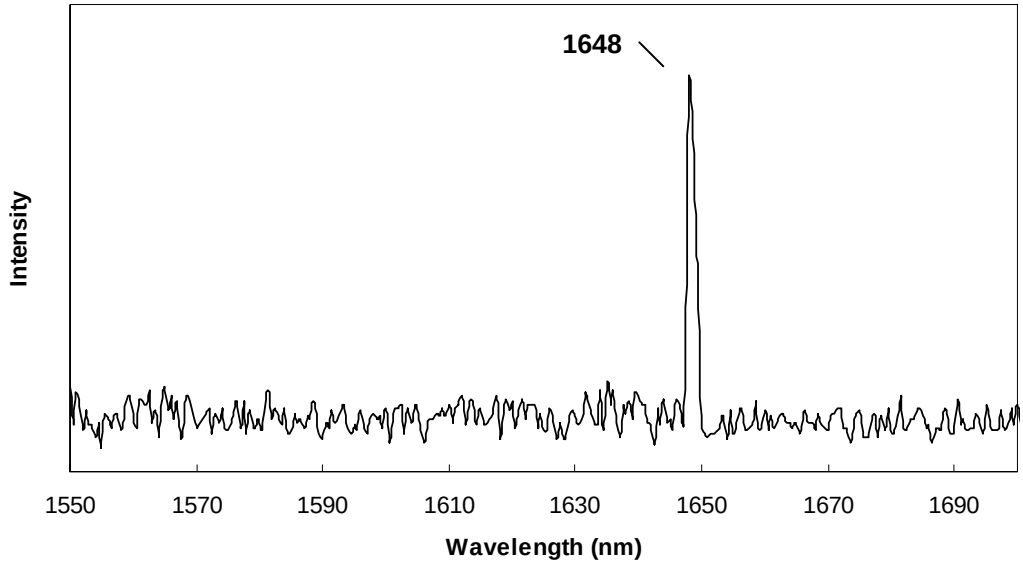

Figure 4.33 The peak refers to G Band of MWNTs.

According to the Raman spectra of the CVD samples produced at 750 °C (figures 4.34-4.36), MWNT peaks were observed at 1596-1598 nm whereas no RBM mode peaks were observed for the SWNTs. This can be due to the large amount of disordered carbon impurities deposited over the SWNTs. The high intensity D-band peaks in these figures (i.e. 1279-1295 nm) show that there is a large amount of disordered carbon deposit over the catalyst particles. Although the samples in figure 4.34 and 4.36 were oxidized at 400°C there were only little differences from the samples without oxidation (i.e. figure 4.35). Probably the carbon deposition time should be lowered in order to decrease the large disordered carbon deposition.

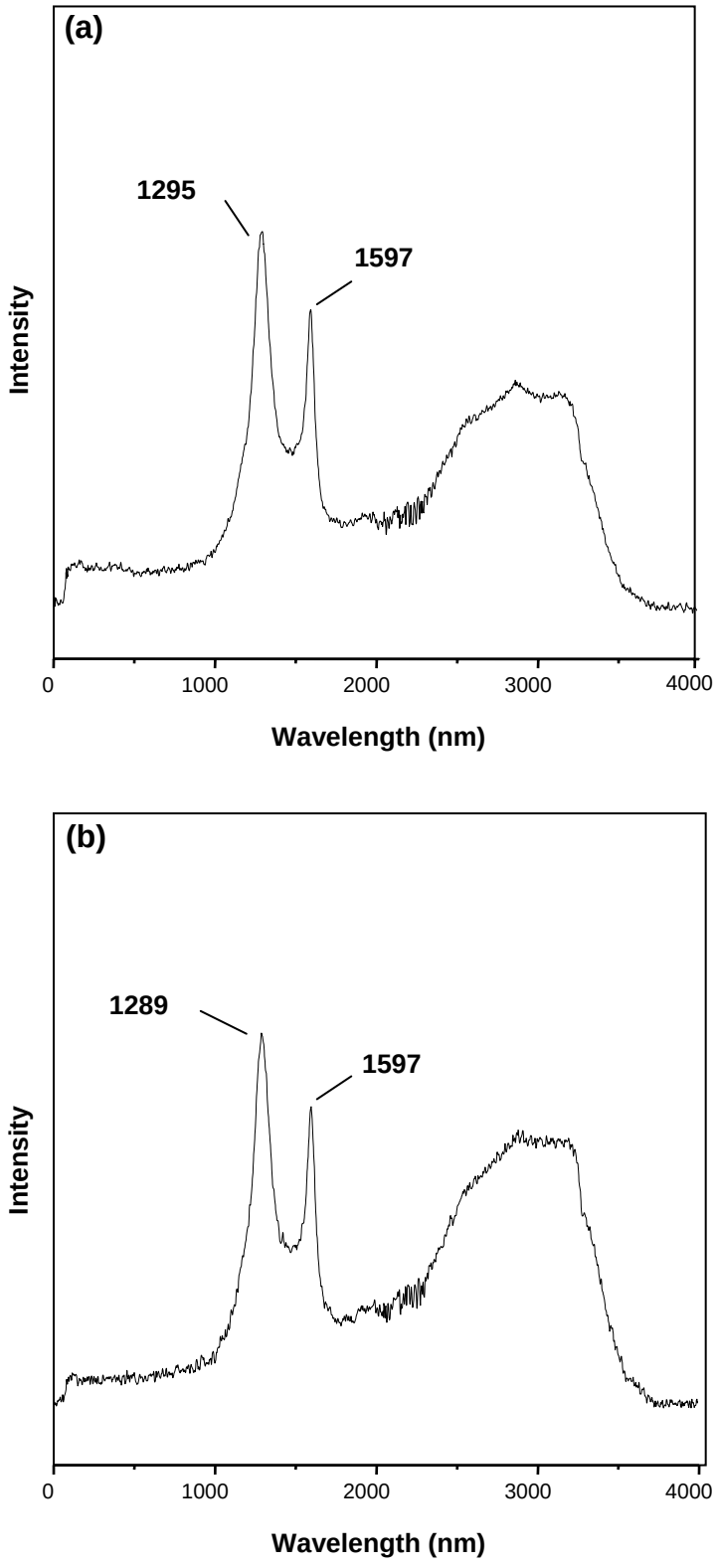

Figure 4.34 Raman results for two 750°C CVD samples on silica plates with 400°C oxidation. Nd: YAG laser was used.

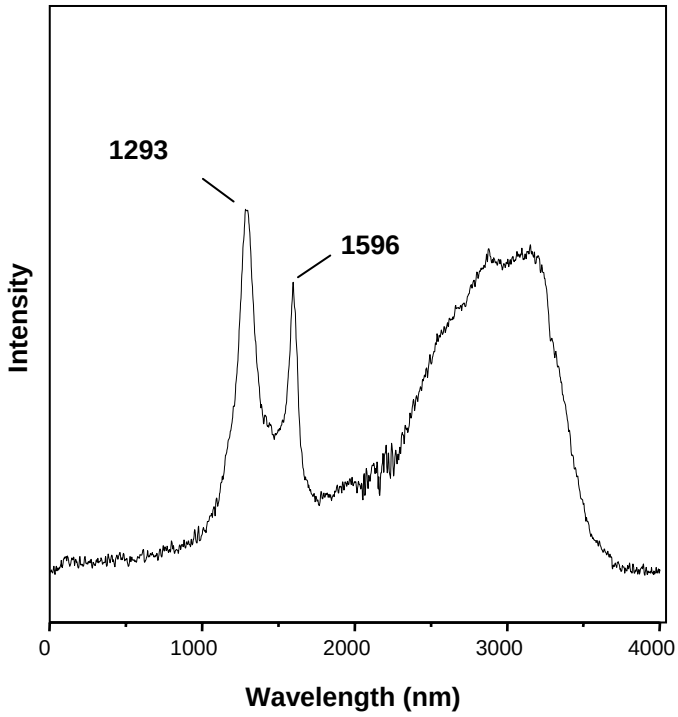

Figure 4.35 Raman spectrum for 750 °C CVD samples.

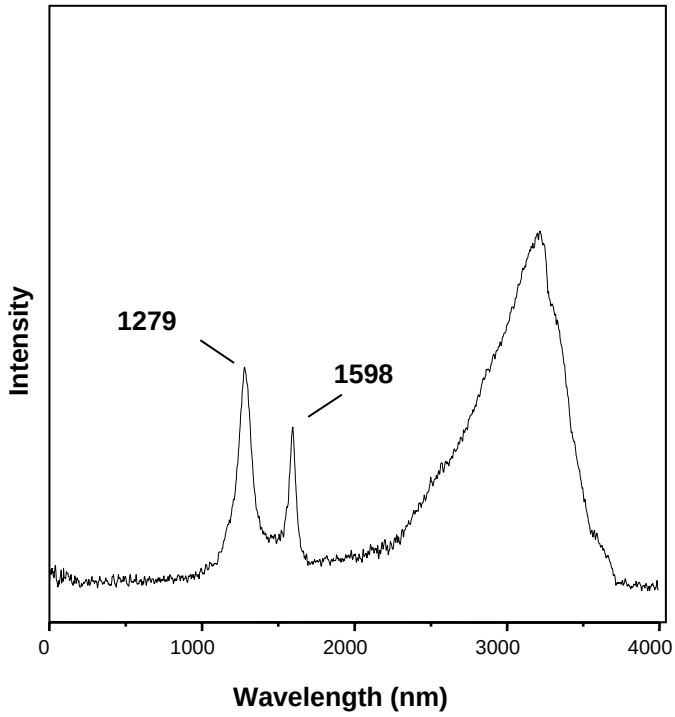

Figure 4.36 Raman result for 750°C CVD powder samples with 400°C oxidation. Nd: YAG laser was used.

CHAPTER 5

CONCLUSIONS

1. The production of carbon nanotubes by both chemical vapor deposition and electron beam methods were achieved successfully.

2. Besides carbon nanotubes, other carbon deposits, possibly fullerene clusters, carbon rods, and onion-like carbon structures were also observed.

3. Nanotubes synthesized by chemical vapor deposition were observed to grow according to the tip-growth model. However, both tip-growth and root-growth mechanisms were effective in electron beam method.

4. Although the TEM images showed multi-walled carbon nanotubes, the Raman spectrum of the substrates from both CVD and e-beam methods showed the existence of single-walled carbon nanotubes. It would have been possible to observe SWNTs if a high resolution TEM were used.

5. In the e-beam method, some nanohorn and bamboo-like structures were also observed in TEM images.

6. In the TEM images of substrates from e-beam method, very big hollow tubular carbon structures were observed that was not reported in the literature before.

7. Nanotubes including catalyst particles and carbon deposits in the tubular channel were observed.

RECOMMENDATIONS

- The analysis should be further carried by High Resolution TEM (300 kV with field emission camera) in order to see smaller sized carbon nanotubes.

- Necessary changes should be made on e-beam device to be able to change experimental parameters (temperature of plasma, vacuum).

- Other carbon containing gases like hydrocarbons can be studied for the nanotube growth.

- Doping of other materials (i.e. Boron) and the resulting structure may be interesting to study.

REFERENCES

1. *"Nanotechnology's unhappy father", The Economist Technology Quarterly,* Vol. 370 No: 8366, p 37, 2004.

2. Kroto, H. W., Heath, J. R., O'Brien, S. C., Curl, R. F., Smalley, R. E., "C_{60}: Buckminsterfullerene", *Nature,* 318, p162, 1985.

3. Iijima, S., "Helical microtubules of graphitic carbon", *Nature*, 354, p56, 1991.

4. William D. Callister, Jr, "Materials Science and Engineering: An Introduction", *New York, John Wiley & Sons*, 2002.

5. Krätschmer, W., Lamb, L. D., Fostiropoulos, K., Huffman, D. R., "Solid C_{60}: a new form of carbon", *Nature,* 347, p354, 1990.

6. Bethune, D. S., Klang, C. H., De Vries, M. S., Gorman, G., Savoy, R., Vazquez, J., Beyers, R., "Cobalt-catalyzed growth of carbon nanotubes with single-atomic-layer walls", *Nature*, 363, p605, 1993.

7. Iijima, S., Ichihashi, T., "Single-shell carbon nanotubes of 1-nm diameter", *Nature*, 363, p603, 1993.

8. Iijima, S., "Nano-aggregates of single-walled graphitic carbon nano-horns", *Chem. Phys. Lett.,* 309, p165, 1999.

9. Iijima, S., "Carbon nanotubes: past, present, and future.", *Physica B*, 323, p1, 2002.

10. Dresselhaus, M. S., Dresselhaus, G., Avouris, Ph., "Carbon Nanotubes: Synthesis, Structure, Properties, and Applications", *Topics in Applied Physics, Springer*, New York, 2001.

11. Saito, R., Dresselhaus, M. S., Dresselhaus, G., "Physical Properties of Carbon Nanotubes", *Imperial College Press,* London, 1998.

12. Cohen, M. L., "Nanotubes, Nanoscience, and Nanotechnology", *Materials Science and Engineering C"*, 15, p1, 2001.

13. Ebbesen, T. W., Ajayan, P. M., “Large-scale synthesis of carbon nanotubes”, *Nature,* 358, p220, 1992.

14. Thess, A., Lee, R., Nikolaev, P., “Crystalline ropes of metallic carbon nanotubes”, *Science,* 273, p483, 1996.

15. Shenderova, O. A., Zhirnov, V. V., Brenner, D. W., ”Carbon Nanostuctures”, *Critical Reviews in Solid State and Materials Sciences,* 27(3/4), p227, 2002.

16. Sinnott, S. B., Andrews, R., Qian, D., Rao, A. M., Mao, Z., Dickey, E.C., Derbyshire, F., “Model of carbon nanotube growth through chemical vapor deposition”, *Chemical Physics Letters*, 315, p25, 1999.

17. Li, W. Z., Xie, S. S., Qian, L. X., Chang, B. H., Zou, B. S., Zhou, W. Y., Zhao, R. A., Wang, G., “Large-Scale synthesis of aligned carbon nanotubes”, *Science,* 274, p1701, 1996.

18. Pan, Z. W., Xie, S. S., Chang, B. H., Zhou, W. Y., Wang, G., “Direct growth of aligned open carbon nanotubes by chemical vapor deposition”, *Chemical Physics Letters,* 299, p97, 1999.

19. Su, M., Zheng, B., Liu, J., “A scalable CVD method for the synthesis of single-walled carbon nanotubes with high catalyst productivity”, *Chemical Physics Letters,* 322, p321, 2000.

20. Lee, C. J., Son, K. H., Park, J., Yoo, J. E., Huh, Y., Lee, J. Y., “Low temperature growth of vertically aligned carbon nanotubes by thermal chemical vapor deposition”, *Chemical Physics Letters,* 338, p113, 2001.

21. Lee, C. J., Lyu, S. C., Cho, Y. R., Lee, J. H., Cho, K. I., “Diameter-controlled growth of carbon nanotubes using thermal vapor deposition”, *Chemical Physics Letters,* 341, p245, 2001.

22. Emmenegger, C., Bonard, J.-M., Mauron, P., Sudan, P., Lepora, A., Grobety, B., Zuttel, A., Schlapbach, L., “Synthesis of carbon nanotubes over Fe catalyst on aluminium and suggested growth mechanism”, *Carbon*, 41, p539, 2003.

23. Kong, J., Cassell, A. M., Dai, H., “Chemical vapor deposition of methane for single-walled carbon nanotubes”, *Chemical Physics Letters,* 292, p567, 1998.

24. Mukhopadhyay, K., Koshio, A., Sugai, T., Tanaka, N., Shinohara, H., Konya, Z., Nagy, J. B., “Bulk production of quasi-aligned carbon

nanotube bundles by the catalytic chemical vapour deposition (CCVD) method", *Chemical Physics Letters,* 303, p117, 1999.

25. Lee, C. J., Park, J., Huh, Y., Lee, J. Y., "Temperature effect on the growth of carbon nanotubes using thermal chemical vapor deposition", *Chemical Physics Letters,* 343, p33, 2001.

26. Lee, C. J., Park, J., Yu, A. J., "Catalyst effect on carbon nanotubes synthesized by thermal chemical vapor deposition", *Chemical Physics Letters,* 360, p250, 2002.

27. Li, W. Z., Wen, J. G., Sennet, M., Ren, Z. F., "Clean double-walled carbon nanotubes synthesized by CVD", *Chemical Physics Letters,* 368, p299, 2003.

28. Hiraoka, T., Kawakubo, T., Kimura, J., et al., "Selective synthesis of double-walled carbon nanotubes by CCVD of acetylene using zeolite supports", *Chemical Physics Letters,* 382, p679, 2003.

29. Hongo, H., Yudasaka, M., Ichihashi, T., Nihey, F., Iijima, S., "Chemical vapor deposition of single-wall carbon nanotubes on iron-film-coated sapphire substrates", *Chemical Physics Letters,* 361, p349, 2002.

30. Strong, K. L., Anderson, D. P., Lafdi, K., Kuhn, J. N., "Purification process for single-wall carbon nanotubes", *Carbon,* 41, p1477, 2003.

31. Pimenta, M. A., Marucci A., Empedocles, S. A., Bawendi, M. G., Hanlon, E. B., Rao, A. M., Eklund, P. C., Smalley, R. E., Dresselhaus, M. S., Dresselhaus, G., "Raman modes of metallic carbon nanotubes", *Physical Review B Rapid Communications"*, vol:58, no:24, 1998.

32. Zhang, H., Chen, K., He, Y., Chen, Y., Wu, C., Wang, J., Liao, J. H., Liu, S. H., "Formation and raman spectroscopy of single wall carbon nanotubes synthesized by CO_2 continuous laser vaporization", *J. Physics and Chemistry of Solids",* 62, p2007, 2001.

33. Dresselhaus, M. S., Dresselhaus, G., Jorio, A., Filho, A. G. S., Saito, R., "Raman spaectroscopy on isolated single wall carbon nanotubes", *Carbon,* 40, p2043, 2002.

34. Okazaki, T., Shinohara, H., "Synthesis and characterization of single-wall carbon nanotubes by hot-filament assisted chemical vapor deposition", *Chemical Physics Letters,* 376, p606, 2003.

35. Bandow, S., Takizawa, M., Hirahara, K., Yudasaka, M., Iijima, S., “Raman scattering study of double-wall carbon nanotubes derived from the chains of fullerenes in single-wall carbon nanotubes”, *Chemical Physics Letters,* 337, p48, 2001.

36. Wei, J., Jiang, B., Zhang, X., Zhu, H., Wu, D., “Raman study on double-walled carbon nanotubes”, *Chemical Physics Letters,* 376, p753, 2003.

37. Gajewski, S., Maneck, H. –E., Knoll, U., Neubert, D., Mach, R., Strauss, B., Friedrich, J. F., ”Purification of single walled carbon nanotubes by thermal gas phase oxidation”, *Diamond and Realted Materials,* 12, p816, 2003.

38. Dillon, A. C., Gennett, T., Jones, K. M., Alleman, J. L., Parilla, P. A., Heben, M. J., “A Simple and Complete Purification of Single-Walled Carbon Nanotube Materials”, *Advanced Materials,* 11 no:6, p1354, 1999.

39. Chiang, I. W., Brinson, B. E., Huang, A. Y., Willis, P. A., Bronikowski, M. J., Margrave, J. L., Smalley, R. E., Hauge, R. H., “Purification and Characterization of Single-Wall Carbon Nanotubes (SWNTs) Obtained from the Gas-Phase Decomposition of CO (HiPco Process)”, *J. Phys. Chem. B***,** 105, p8297, 2001.

40. Chiang, I. W., Brinson, B. E., Smalley, R. E., Huang, A. Y., Margrave, J. L., Hauge, R. H., “Purification and Characterization of Single-Wall Carbon Nanotubes”, *J. Phys. Chem. B***,** 105, p1157, 2001.

41. Tans S. J., Verschueren, A. R. M., Dekker, C., “Room-temperature transistor based on a single carbon nanotube”, *Nature,* 393, p49, 1998.

42. Wei, B. Q., Vajtai, R., Ajayan, P. M., “Reliability and current carrying capacity of carbon nanotubes”, *Applied Physics Letters,* 79, p1172, 2001.

43. *NEC Corporation Press Release,* September 2003.

44. Hone, J., *Carbon Nanotube Topics in Applied Physics,* 273, 2001.

45. Cengel, Y. A., “Heat Transfer: A practical Approach”, *McGraw-Hill,* New York, 1998.

46. Shi, L., “Thermal Properties of Materials”, Department of Mechanical Engineering & Center for Nano and Molecular Science & Technology, Texas Materials Institute The University of Texas at Austin, TX 78712, www.me.utexas.edu/~lishi/Bootcamp_Shi.ppt, 2003.

47. Treacy, M. M., Ebbesen, T. W., Gibson, J. M., “Exceptionally high Young’s modulus observed for individual carbon nanotubes”, *Nature* (38), p678, 1996.

48. Treacy, M. M., Ebbesen, T. W., et. al., “Young’s Modulus of SWNTs”, *Physical Review B*, 58, p20, 1998.

49. Yu, M. F., Lourie, O., Dyer, M.J., Moloni, K., Kelly, T. F., Ruo, R. S., “Strength and breaking mechanism of multiwalled carbon nanotubes under tensile load”, *Science,* 287, (5453), p637, 2000.

50. Pantano, A., Parks, D. M., Boyce, M. C., “Mechanics of deformation of single- and multi-wall carbon nanotubes”, *Journal of the Mechanics and Physics of Solids*, 52, p789, 2004.

51. Wikipedia Internet Encyclopedia, www.wikipedia.com .

52. Schreuder-Gibson, H., Senecal, K., Sennett, M., Huang, Z., et al., “Characteristics of electrospun carbon nanotube-polymer composites”, *Nanolab,* 2003.

53. Glatkowski, P. J., “Carbon nanotube based transparent conductive coatings”, *Eikos Inc., 2 Master Drive, Franklin, MA. 02038,* 2003.

54. “IBM creates the worlds highest performing nanotube transistor”, *IBM Research News,* May 20, 2002.

55. Li, S., Yu, Z., Yen, S., Tang, W. C., Burke, P. J., “Carbon Nanotube Transistor Operation at 2.6 GHz”, *Nano Letters,* vol:4 no:4, p753, 2004.

56. “NEC uses Carbon Nanotubes to Develop a Tiny Fuel Cell for Mobile Applications”, *NEC Press Release*, 2001.

57. Gao, B., Bower, C., Lorentzen, J. D., Fleming, L., Kleinhammes, A. Tang, X. P., McNeil, L. E., Wu, Y., Zhou, O., “Enhanced saturation lithium composition in ball-milled single-walled carbon nanotubes”, *Chemical Physics Letters,* 327, p69, 2000.

58. Ma, R. Z., et al., *Science in China Series E-Technological Sciences,* 43, p178, 2000.

59. Novak, J. P., Snow, E. S., Houser, E. J., Park, D., Stepnowski, J. L., McGill, R. A., “Nerve agent detection using networks of single-walled carbon nanotubes”, *Applied Physics Letters,* vol:83 no:19, p4026, 2003.

60. David, L., “The Space Elevator Comes Closer to Reality”, www.space.com/businesstechnology/technology/space_elevator_020327-1.html, 2002

61. Goktas, H., Oke, G., Udrea, M., Kirkici, H., “Micro Processing by Intense Fast Electron Beam”, *IEEE Transaction on Plasma Science*, vol. 50, No. 5, p1837, 2002.